

High-Performance Analog Products

Analog Applications Journal

Second Quarter, 2006



IMPORTANT NOTICE

Texas Instruments Incorporated and its subsidiaries (TI) reserve the right to make corrections, modifications, enhancements, improvements, and other changes to its products and services at any time and to discontinue any product or service without notice. Customers should obtain the latest relevant information before placing orders and should verify that such information is current and complete. All products are sold subject to TI's terms and conditions of sale supplied at the time of order acknowledgment.

TI warrants performance of its hardware products to the specifications applicable at the time of sale in accordance with TI's standard warranty. Testing and other quality control techniques are used to the extent TI deems necessary to support this warranty. Except where mandated by government requirements, testing of all parameters of each product is not necessarily performed.

TI assumes no liability for applications assistance or customer product design. Customers are responsible for their products and applications using TI components. To minimize the risks associated with customer products and applications, customers should provide adequate design and operating safeguards.

TI does not warrant or represent that any license, either express or implied, is granted under any TI patent right, copyright, mask work right, or other TI intellectual property right relating to any combination, machine, or process in which TI products or services are used. Information published by TI regarding third-party products or services does not constitute a license from TI to use such products or services or a warranty or endorsement thereof. Use of such information may require a license from a third party under the patents or other intellectual property of the third party, or a license from TI under the patents or other intellectual property of TI.

Reproduction of information in TI data books or data sheets is permissible only if reproduction is without alteration and is accompanied by all associated warranties, conditions, limitations, and notices. Reproduction of this information with alteration is an unfair and deceptive business practice. TI is not responsible or liable for such altered documentation.

Resale of TI products or services with statements different from or beyond the parameters stated by TI for that product or service voids all express and any implied warranties for the associated TI product or service and is an unfair and deceptive business practice. TI is not responsible or liable for any such statements.

Following are URLs where you can obtain information on other Texas Instruments products and application solutions:

Products

Amplifiers	amplifier.ti.com
Data Converters	dataconverter.ti.com
DSP	dsp.ti.com
Interface	interface.ti.com
Logic	logic.ti.com
Power Management	power.ti.com
Microcontrollers	microcontroller.ti.com

Applications

Audio	www.ti.com/audio
Automotive	www.ti.com/automotive
Broadband	www.ti.com/broadband
Digital control	www.ti.com/digitalcontrol
Military	www.ti.com/military
Optical Networking	www.ti.com/opticalnetwork
Security	www.ti.com/security
Telephony	www.ti.com/telephony
Video & Imaging	www.ti.com/video
Wireless	www.ti.com/wireless

Mailing Address: Texas Instruments
Post Office Box 655303
Dallas, Texas 75265

Contents

Introduction	4
Data Acquisition	
Matching the noise performance of the operational amplifier to the ADC	5
Selecting an op amp to drive a SAR ADC requires evaluation of many parameters. Device noise is easy to overlook but can have a dramatic effect on system performance. This article describes how device noise specifications can be used to predict system SNR so that the effects of amplifier noise have minimal impact on ADC operation.	
Power Management	
TLC5940 PWM dimming provides superior color quality in LED video displays	10
High-quality LED video displays require dot correction to equalize the brightness variation of all LEDs in the display. This article describes PWM-dimming techniques that permit three primary-color LEDs to produce millions of colors.	
Wide-input dc/dc modules offer maximum design flexibility	13
Wide-input nonisolated power modules like the TI PTN78 series offer cost-effective dc/dc power supply solutions. With typical input voltage ranges between 7 and 36 V, these modules are compact and easy to use; and they can simplify inventory requirements because they can be used in a variety of system and portable applications.	
Powering today's multi-rail FPGAs and DSPs, Part 2	18
This article provides recommendations and guidance for developing a power solution for multi-rail applications. It focuses on how to choose between the types of point-of-load dc/dc converters and how to design them to meet dc accuracy, start-up, and transient requirements.	
Interface (Data Transmission)	
Device spacing on RS-485 buses	25
RS-485 bus distributed inductance and capacitance are determined by PCB traces, interconnecting cable(s), connectors, terminators, and RS-485 devices added along the bus. Analysis in this article derives a guideline for spacing RS-485 nodes along a bus segment.	
Amplifiers: Op Amps	
Low-cost current-shunt monitor IC revives moving-coil meter design	27
Moving-coil meters are still preferred in many applications. Using meters in applications with very low signal current is easily accomplished with modern current-shunt monitor ICs like those in the TI INA19x family. This article describes the typical operation of INA19x current-shunt monitors when they are used in meter control circuitry.	
Index of Articles	30
TI Worldwide Technical Support	33

To view past issues of the
***Analog Applications Journal*, visit the Web site**
www.ti.com/aaj

Introduction

Analog Applications Journal is a collection of analog application articles designed to give readers a basic understanding of TI products and to provide simple but practical examples for typical applications. Written not only for design engineers but also for engineering managers, technicians, system designers and marketing and sales personnel, the book emphasizes general application concepts over lengthy mathematical analyses.

These applications are not intended as “how-to” instructions for specific circuits but as examples of how devices could be used to solve specific design requirements. Readers will find tutorial information as well as practical engineering solutions on components from the following categories:

- Data Acquisition
- Power Management
- Interface (Data Transmission)
- Amplifiers: Op Amps

Where applicable, readers will also find software routines and program structures. Finally, *Analog Applications Journal* includes helpful hints and rules of thumb to guide readers in preparing for their design.

Matching the noise performance of the operational amplifier to the ADC

By **Bonnie C. Baker** (Email: bonnie@ti.com)

Senior Applications Engineer

Proper selection of the operational amplifier that drives an analog-to-digital converter (ADC) in a mixed-signal application is critical. The designer must compare issues such as amplifier noise, bandwidth, settling time, and slew rate to the ADC's signal-to-noise ratio (SNR), spurious-free dynamic range (SFDR), input impedance, and sampling time. This article specifically addresses the matching of the noise specifications and performance of an op amp and a successive approximation register (SAR) ADC in a single-supply environment.

The noise that the amplifier generates originates from the input differential stage. The input stage of every amplifier generates transistor-device noise, which spot-noise graphs describe as referred-to-input (RTI) noise. With this graphical information we can determine how much noise reaches the input terminal of the ADC by calculating the referred-to-output (RTO) amplifier noise.

This discussion begins with a description of the amplifier's device noise. The amplifier noise sources are then tied together into one figure of merit, and the units are

converted from volts to an SNR in decibels. Finally, the impact of the op amp in this mixed-signal circuit (Figure 1) is determined by calculating the combination of the op amp SNR value with the ADC's SNR performance.

Characteristics of the amplifier noise

It is important to understand the noise that the operational amplifier generates in this application. The typical performance of the amplifier given in its product datasheet shows that the op amp noise behavior over frequency has a signature that is unmistakable (see Figure 2). In this article, since we will consider the effects of using a single-supply CMOS amplifier, the input current noise is low enough that we can ignore it. Here we will consider only the effects of the amplifier's voltage noise.

The amplifier noise specification in the typical amplifier datasheet is an RTI specification. We can model the amplifier noise as a voltage source at the non-inverting input of the amplifier. The electrical characteristics table of an operational amplifier gives the input voltage noise

Figure 1. Typical driver circuit for SAR ADC

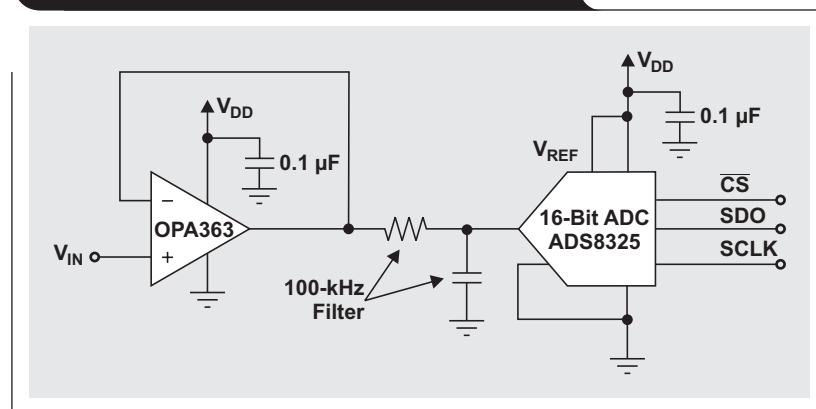
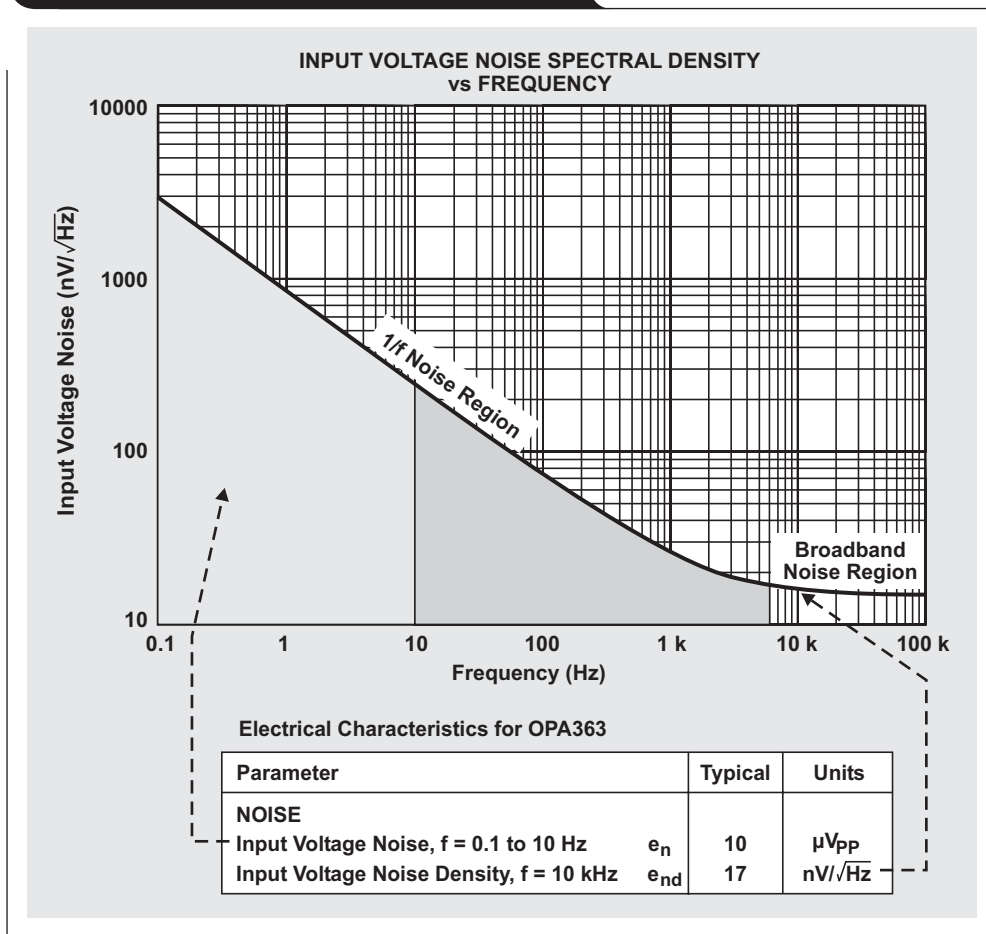


Figure 2. OPA363 amplifier noise parameters



and input voltage noise density specifications (see Figure 2). The input voltage noise specification ($10 \mu\text{V}_{PP}$) describes the low-frequency noise of the amplifier in terms of a bandwidth. This bandwidth is part of the 1/f noise region of the amplifier. The transistors in the input stage of the amplifier, along with the input-stage active load, generate this noise.

Input voltage noise density calls out a noise figure that refers to one frequency. For instance, the electrical characteristics table in Figure 2 shows that the input voltage noise density (e_{nd}) at 10 kHz is equal to $17 \text{ nV}/\sqrt{\text{Hz}}$. Usually this specification appears in the broadband-noise portion of the frequency plot (Figure 2). Theoretically, this broadband noise is flat. Assuming that it is flat is a good estimate of the amplifier's behavior. The resistors inside the operational amplifier primarily generate the broadband noise whether they are diffused resistors or the source and drain of the transistors.

The amplifier datasheet contains a typical specification graph that shows the input voltage noise density versus frequency. Figure 2 is an example of this type of graph. In this example, the input voltage noise specification is equal to the area beneath the input-voltage, noise-density curve

between the specified frequencies of 0.1 and 10 Hz. Note that the units for this specification are peak-to-peak. To convert this to an rms value, simply divide the peak-to-peak value by 6.6 (industry-standard crest factor [CF] = 3.3).

Table 1 contains typical CF values used to convert rms to peak-to-peak values (and vice versa). To estimate the peak-to-peak operational amplifier output noise voltage, multiply the rms output voltage by $2 \times \text{CF}$. To estimate the ADC peak-to-peak output bit performance, subtract the bit crest factor (BCF) from the rms specification.

Table 1. Crest factor and bit crest factor values used for conversions from rms to peak-to-peak

CREST FACTOR (CF) (V)	BIT CREST FACTOR (BCF) (Bits)	ADC CONVERSIONS WITHIN THE PEAK-TO-PEAK LEVELS (%)
2.6	2.38	99
3.3*	2.72	99.9
3.9	2.96	99.99
4.4	3.14	99.999
4.9	3.29	99.9999

*Industry standard

We can easily calculate the noise underneath the curve in Figure 2 for different input voltage noise bandwidths in the 1/f region. The first order of business in this calculation is to determine the input noise density at 1 Hz. Once we find that value, the following simple formula will provide the rms noise under the curve.

$$V_{(1/f): f1-f2} = C \sqrt{\ln\left(\frac{f_2}{f_1}\right)},$$

where C is equal to the input noise density at 1 Hz.

As an example, the amount of rms noise produced by the amplifier shown in Figure 2 from 0.1 Hz to 6000 Hz is:

$$V_{(1/f): f1-f2} = C \sqrt{\ln\left(\frac{f_2}{f_1}\right)},$$

$$V_{(1/f): f1-f2} = 700 \text{ nV} \sqrt{\ln\left(\frac{6000}{0.1}\right)}, \text{ and}$$

$$V_{(1/f): f1-f2} = 2.32 \text{ } \mu\text{V}_{\text{rms}}.$$

With this calculation, and with the amplifier noise gain $G = 1$, the SNR at the output of the amplifier for the 1/f noise is:

$$\text{SNR}_{\text{OPA}} = 20 \log_{10} \left(\frac{V_{\text{OUT-rms}}}{G \times V_{(1/f): f1-f2}} \right),$$

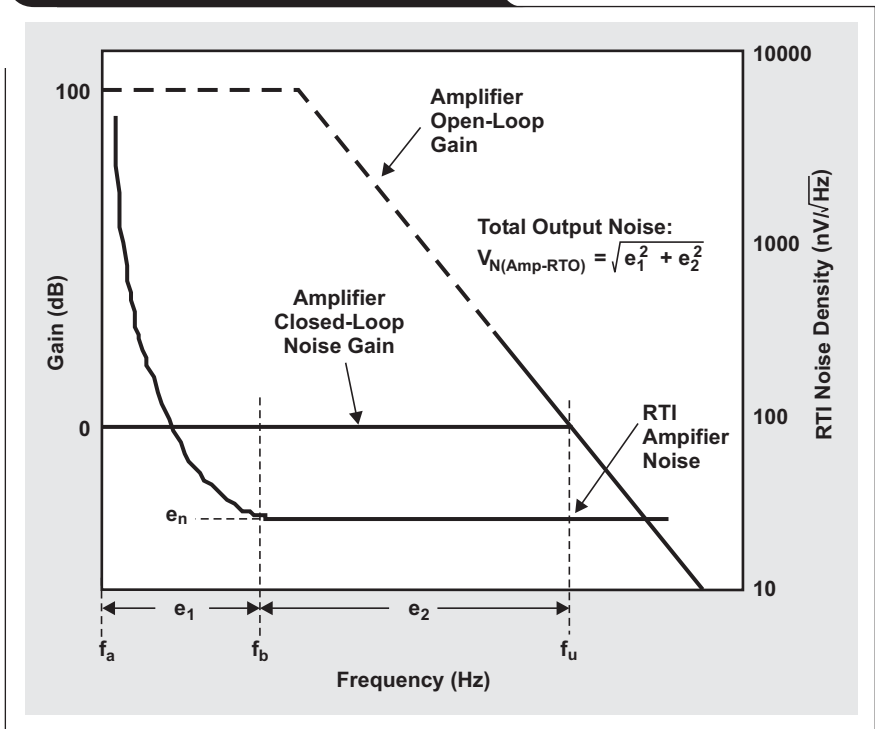
$$\text{SNR}_{\text{OPA}} = 20 \log_{10} \left(\frac{5 \text{ V}}{2\sqrt{2} \times 2.32 \text{ } \mu\text{V}} \right), \text{ and}$$

$$\text{SNR}_{\text{OPA}} = 117.6 \text{ dB}.$$

When we think about noise at these low frequencies, we may jump to the conclusion that we should take this formula down to a very low frequency, such as 0.0001 Hz (0.0001 Hz = 1 cycle per 2.8 hours). However, at frequencies lower than 0.1 Hz, which is one cycle every 10 seconds, it is very possible that other things such as temperature, aging, or component life are changing in the circuit. Realistically, low-frequency noise from the amplifier will probably not appear at this sample speed; but changes in the circuit, such as temperature or power supply voltage, may.

The amplifier table of specifications (Figure 2) also gives the input noise density value. This specification is always at a higher frequency, in the area where the input voltage noise is relatively constant. For this region of the curve, multiplying the square root of the bandwidth and the noise density derives the noise across this bandwidth. For example, if the noise of the amplifier is 17 nV/ $\sqrt{\text{Hz}}$ at

Figure 3. Typical RTI noise evaluation



10 kHz, the noise from the amplifier across the bandwidth of 6 kHz to 100 kHz is:

$$V_{1-100 \text{ kHz}} = (\text{Noise Density at 10 kHz})\sqrt{\text{BW}},$$

$$V_{1-100 \text{ kHz}} = e_{\text{nd}}\sqrt{\text{BW}},$$

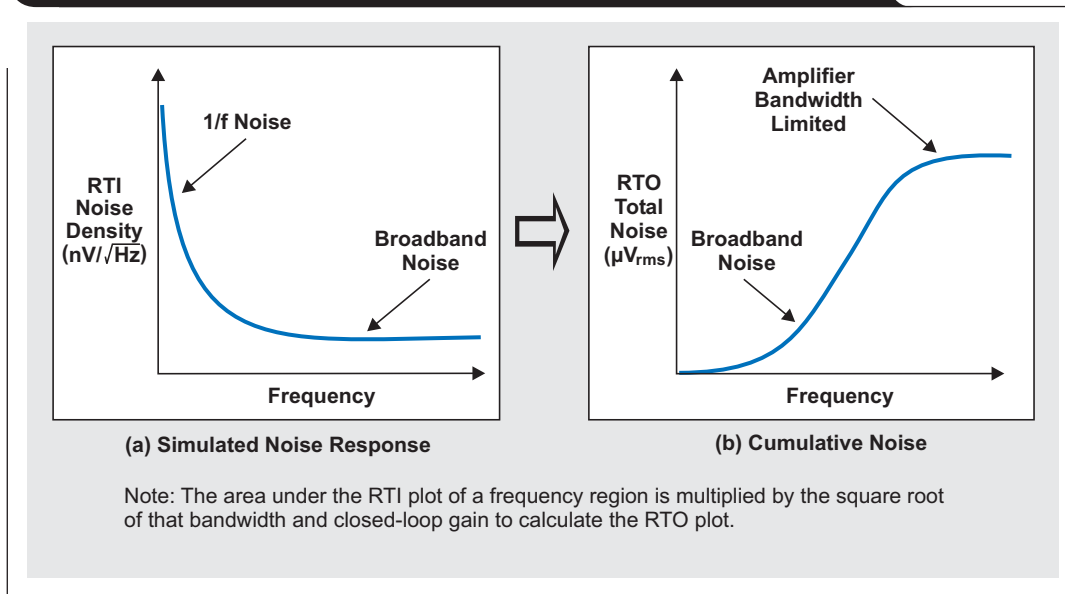
$$V_{1-100 \text{ kHz}} = (17 \text{ nV}/\sqrt{\text{Hz}})(\sqrt{100,000 - 1,000}), \text{ and}$$

$$V_{1-100 \text{ kHz}} = 5.21 \text{ } \mu\text{V}_{\text{rms}},$$

where BW is equal to the bandwidth of interest.

So how do we get from the manufacturer's graph to an RTO noise value? We calculate the area beneath the noise curve and multiply that times the noise gain of the amplifier. In this example, the noise gain of our circuit is +1 V/V. We determine the noise that the amplifier contributes in both regions and then add the two values together using the square root of the sum of the squares. Figure 3 shows the formula for this calculation and illustrates the two regions.

Figure 3 separates the noise into two parts. In region e_1 , we gain the 1/f noise of the amplifier by the dc gain of the amplifier circuit, which is +1 V/V. The specifications for amplifier noise are in nanovolts per square root of hertz. So the analysis is complete when we multiply the average noise over the region by the square root of the bandwidth of that region. For CMOS amplifiers, the 1/f region is usually from 0.1 Hz to 100 Hz up to 1000 Hz. Since this noise value is multiplied by the square root of the bandwidth, its

Figure 4. Graphical representation of RTI noise density and RTO noise

contribution is low. In region e_2 , the broadband noise of the amplifier is multiplied by the amplifier circuit gain, which is again +1 V/V, and the square root of the bandwidth.

Each region contributes to the overall circuit noise:

$$e_1 = C \sqrt{\ln\left(\frac{f_b}{f_a}\right)} = 2.32 \mu\text{Vrms}$$

$$e_2 = e_n \sqrt{f_2 - f_1} = 5.21 \mu\text{Vrms}$$

The total noise at the output of the amplifier is:

$$\begin{aligned} V_{N(\text{Amp-RTO})} &= \sqrt{e_1^2 + e_2^2} \\ &= 5.70 \mu\text{Vrms}. \end{aligned}$$

With this calculation, the SNR at the output of the amplifier for the 1/f noise is:

$$\text{SNR}_{\text{OPA}} = 20 \log_{10} \left(\frac{V_{\text{OUT-rms}}}{V_{N(\text{Amp-RTO})}} \right),$$

$$\text{SNR}_{\text{OPA}} = 20 \log_{10} \left(\frac{5 \text{ V}}{5.70 \mu\text{V}} \right), \text{ and}$$

$$\text{SNR}_{\text{OPA}} = 109.8 \text{ dB}.$$

We can validate this noise calculation using the Texas Instruments (TI) SPICE simulation tool, TINA-TI™. This tool can be found at amplifier.ti.com under “Engineering Resources.”

The two graphs in Figure 4 demonstrate how TINA-TI can help us understand the noise in our circuit. Figure 4(a) shows the simulated noise response of an amplifier. Figure 4(b) provides the cumulative noise as frequency increases. Notice that the noise is very low at the lower frequencies in Figure 4(b). This is because the lower bandwidths are multiplied by the square root of a small number, the bandwidth. As frequency increases, the cumulative noise also increases. One would think that at higher frequencies the increases in noise would be less because of the characteristics of Figure 4(a). As we can see, this is not true, because the bandwidth multiplier (square root of the bandwidth) is larger at higher frequencies.

Combining the op amp and ADC noise figures

Once we examine the amplifier for possible noise sources, it is easy to evaluate the total noise of the system in Figure 1. This system uses the 16-bit ADC, ADS8325, whose maximum sample rate is 100 ksp/s. The typical SNR of this device is 91 dB.

As we found before, the OPA363 RTO noise is 109.8 dB. Now we can determine the total noise of the system by using the op amp SNR and ADC SNR, and applying the theorem of taking the square root of the sum of the squares.

$$\text{SNR}_{\text{Total}} = -20 \log_{10} \sqrt{10^{-\text{SNR}_{\text{Op Amp}}/10} + 10^{-\text{SNR}_{\text{ADC}}/10}}$$

$$\text{SNR}_{\text{Total}} = 90.94 \text{ dB}$$

From this calculation we can see that the amplifier noise has very little impact on the resolution of the system.

With the devices in the circuit, the SNR performance will always be equal to or less than the lowest value. Given this interaction between the amplifier and ADC, picking a higher-noise amplifier will give the worst results. For instance, if we use an amplifier in a gain of 10 V/V that has a typical voltage noise specification of $e_{nd} = 45 \text{ nV}/\sqrt{\text{Hz}}$ at 10 kHz, then $\text{SNR}_{\text{Total}}$ is 82.2 dB. If we use the 16-bit ADS8325, then $\text{SNR}_{\text{Total}}$ is 81.6 dB. In this example, the amplifier is dominating the noise of the circuit.

There are more factors that have an effect on the amplifier selection process, but amplifier noise can have a significant effect on the digital code outcome. If the amplifier is too noisy, the ADC will reliably convert the noise from the amplifier circuit to the digital output. On the other hand, it is possible to have an ADC that is noisier than the amplifier circuit. If we choose an extremely low-noise amplifier without evaluating the system, we will probably spend too much money on one component or the other. Determining the potential noise in a circuit is always a daunting challenge, but there are some general rules of thumb that can be applied to overcome these problems. We can use the circuit's frequency range to our advantage in the calculations; and, when we combine noise sources, we can use the equation for the square root of the sum of the squares. By using these tricks we can quickly determine the compatibility of our amplifier/ADC combination.

In this circuit an amplifier isolates impedances in the signal chain. Other features, like gain or filtering, can be added; but regardless of the features we put around the amplifier, we should always ensure that the amplifier circuit preserves the integrity of the ADC.

References

For more information related to this article, you can download an Acrobat Reader file at www-s.ti.com/sc/techlit/litnumber and replace "litnumber" with the **TI Lit. #** for the materials listed below.

Document Title	TI Lit. #
1. "1.8V, 7MHz, 90dB CMRR, Single-Supply, Rail-to-Rail I/O Operational Amplifier," OPA363/2363, OPA364/2364, OPA4364 Datasheetsbos259
2. Bonnie Baker, <i>A Baker's Dozen: Real Analog Solutions for Digital Designers</i> (Newnes-Elsevier, 2005).	—
3. Howard Johnson and Martin Graham, <i>High-speed Digital Design: A Handbook of Black Magic</i> (Prentice-Hall, 1993).	—
4. Henry Ott, <i>Noise Reduction Techniques in Electronic Systems</i> (New York: John Wiley, 1998).	—
5. <i>The RF Capacitor Handbook</i> (American Technical Ceramics Inc.).	—
6. Tim Williams, <i>The Circuit Designer's Companion</i> , 2nd ed. (Newnes-Elsevier, 2005).	—
7. Edward C. Jordan, Ed., <i>Reference Data for Engineers: Radio, Electronics, Computer & Communications</i> , 7th ed. (Sams, 1985).	—

Related Web sites

dataconverter.ti.com

www.ti.com/sc/device/ADS8325

www.ti.com/sc/device/OPA363

For more information on TI's SPICE simulation tool, TINA-TI, and TI's FilterPro™ Active Filter Design software, please visit amplifier.ti.com

TLC5940 PWM dimming provides superior color quality in LED video displays

By Michael Day (Email: m-day@ti.com)

Applications Manager, Portable Power Products

A design technique called dot correction was discussed in Reference 1. This technique is used to calibrate each individual pixel in large form-factor displays. Once calibrated, or dot corrected, each pixel provides the same brightness level when commanded to a specific brightness. This technique calibrates the analog current supplied through individual LEDs in an array. While dot correction offers an excellent solution that compensates for the variation of lumen output between pixels, this analog brightness adjustment is only the first step in developing a high-quality LED display. This article presents a technique called pulse width modulation (PWM) dimming that can be used to adjust LED brightness while maintaining superior color quality. This technique is also referred to as PWM grayscale.

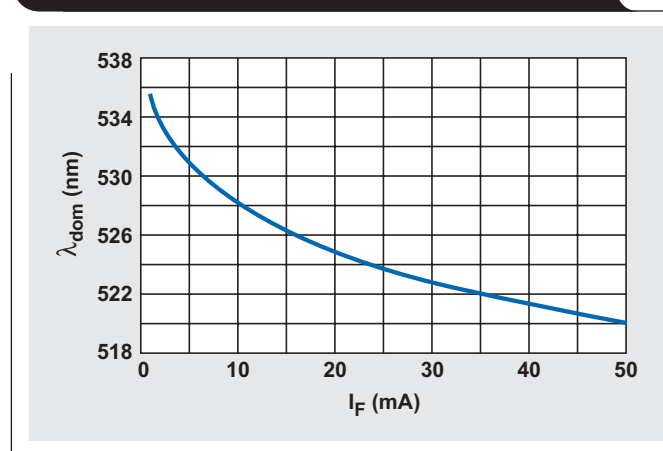
Low-end displays typically require only monochromatic LEDs. Applications include simple sporting scoreboards, single-line scrolling displays, and transportation road signs. A newer and growing market requires high-quality video displays capable of full-motion video shown in millions of colors. These applications include ever-expanding advertising markets encompassing convenience stores, shops, gas stations, and stadiums. An emerging market for LEDs is in DLP- and LCD-based televisions. Accurate color reproduction in these televisions is dependent on the available colors in the backlight. Proper control of the red, green, and blue (RGB) LEDs produces a color spectrum that is larger than the NTSC color space for television broadcasts. By contrast, cold cathode fluorescent lamp (CCFL) backlighting only produces about 85% of the NTSC color spectrum.

These displays require sophisticated LED drivers capable of providing multiple brightness levels. The number of colors available in the display is proportional to the number of brightness levels available for each of the RGB LEDs that make up a single pixel in the overall display. Competition between display manufacturers is driving designers toward high-end LED drivers with integrated PWM functionality capable of delivering thousands of brightness levels. These brightness levels result in enhanced color shading and improved video quality. The TLC5940 is designed to meet these needs.

High-quality, full-color video requires hundreds or thousands of brightness levels between 0% and 100%. Older LED drivers use analog dimming to provide these brightness levels. Analog dimming changes brightness by changing the LED's forward current. For example, if an LED is at full brightness with 20 mA of forward current, then 25% brightness is achieved by driving the LED with 5 mA of forward current. While this dimming scheme is simple and works well for lower-end displays, the drawback with analog dimming is that an LED's color shifts with changes in forward current. Figure 1 shows a true green LED's color variation with changes in forward current. This LED's full brightness is specified at 20 mA. Analog dimming to 25% brightness shifts the color spectrum from 525 nm to 531 nm. This color shift becomes unacceptable in displays requiring a true color representation.

PWM dimming provides reduced brightness by modulating the LED's forward current between 0% and 100%. The LED brightness is controlled by adjusting the relative ratios

Figure 1. Color shift caused by analog dimming



of the on time and off time. A 25% brightness level is achieved by turning the LED on at full current for 25% of each period. Figure 2 shows a comparison between analog and PWM dimming for a 20-mA LED being dimmed to 25% brightness. To keep the user from seeing the LED turn on and off, the switching speed must be greater than 100 Hz. Above 100 Hz, the human eye averages the on and off times, seeing only an effective brightness that is proportional to the LED's on-time duty cycle. The advantage of PWM dimming is that the forward current is always constant, so LED color does not vary with brightness like it does with analog dimming. Pulsing the current provides precise brightness control while preserving the color purity.

Since this type of PWM dimming is microprocessor-driven, it is limited to a maximum number of discrete brightness levels, commonly referred to as grayscale steps, for each LED. The total available number of discrete steps during any one period determines the LED's brightness resolution. High-quality displays require hundreds to thousands of brightness steps to accurately reproduce the full color spectrum necessary for full-motion video. The TLC5940 provides 12 bits of PWM dimming to meet this need. These 12 bits of resolution provide $2^{12} = 4096$ shades for each LED. Each pixel in a color display is composed of three LEDs—red, green, and blue. Individually driving each of these LEDs to one of 4096 brightness levels renders the RGB cluster capable of 68.7 billion colors.

The following example illustrates the TLC5940 PWM dimming capabilities. For simplicity, the example assumes there are only 3 bits of PWM dimming. Since 3 bits is equivalent to $2^3 = 8$ shades, each LED can be programmed to stay on anywhere from 0 to 7 PWM grayscale steps. Each video frame starts with all LEDs turned off. At the rising edge of the first PWM clock, all LEDs turn on except ones that are programmed with grayscale values of zero. The IC increments a grayscale counter at the beginning of each PWM clock cycle. Each LED stays on until the PWM grayscale counter goes above the LED's programmed PWM value. This is better explained by Figure 3, which shows waveforms and a block diagram for a simplified 3-bit PWM dimming controller. Programming the grayscale value of the red, green, and blue

Figure 2. Analog dimming vs. PWM dimming

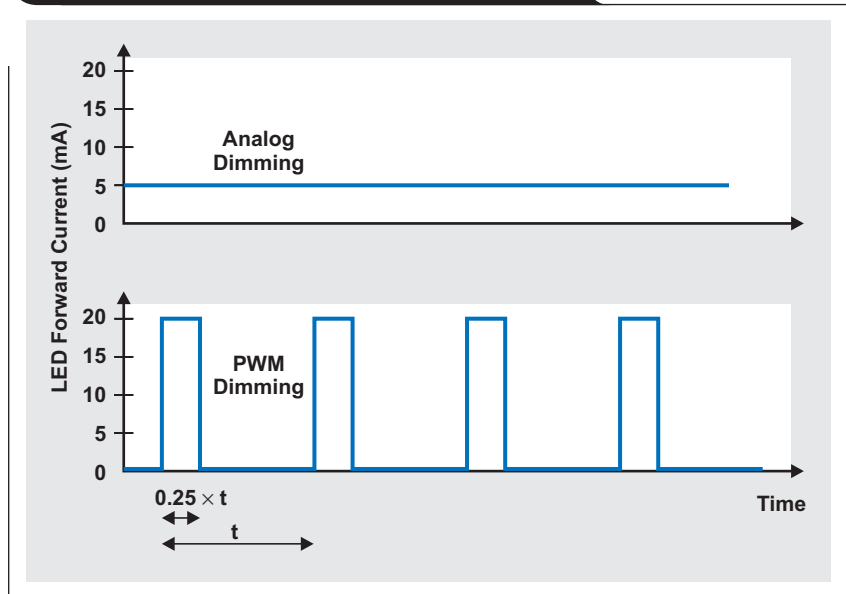


Figure 3. Orange pixel generated with 3-bit PWM dimming

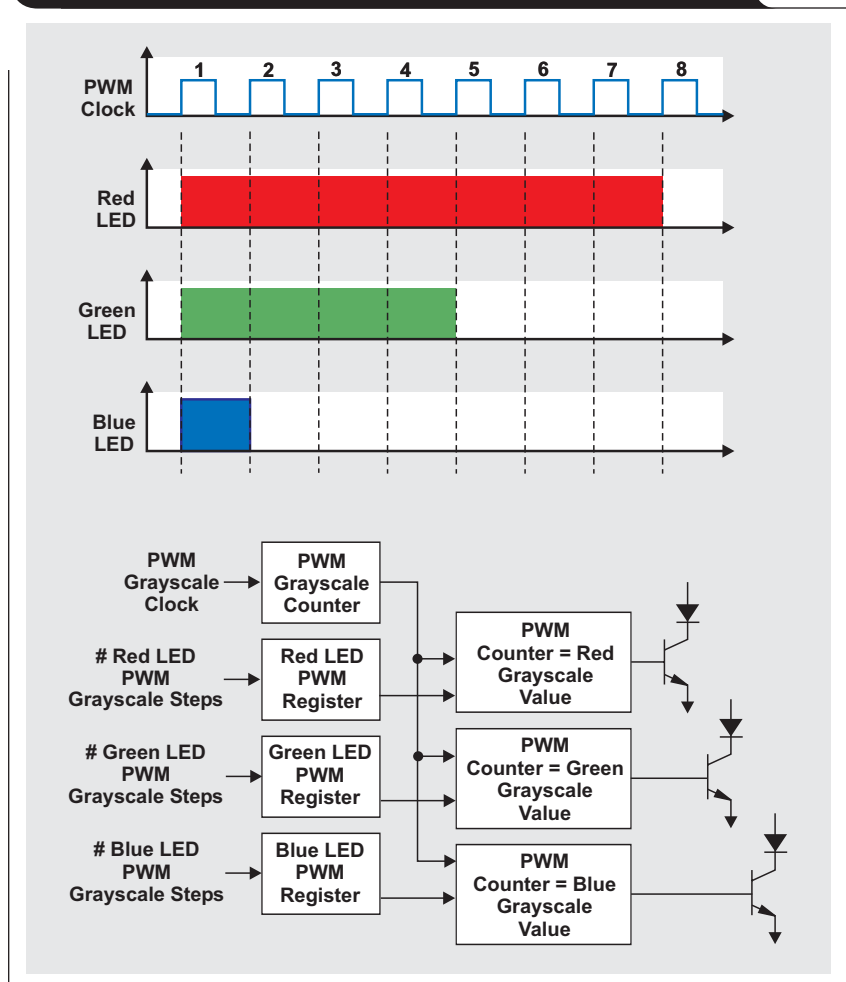
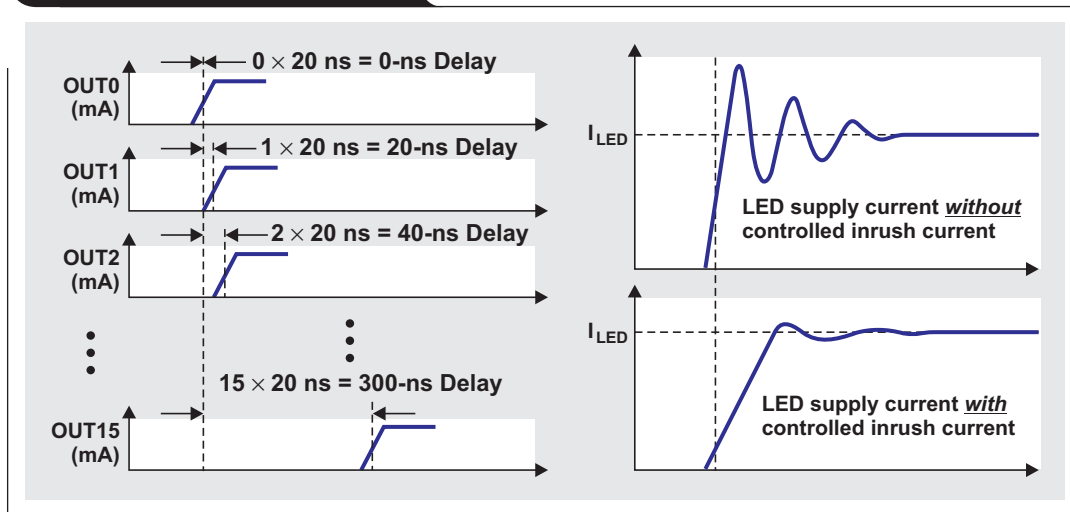


Figure 4. Inrush current control



LEDs to 7, 4, and 1, respectively, produces an orange pixel on the screen. The green LED is programmed to a grayscale value of 4. It turns on at the rising edge of the first PWM clock cycle and stays on for four full PWM clock cycles. This 3-bit PWM dimming example is capable of producing $2^3 \times 2^3 \times 2^3 = 512$ colors for each RGB pixel. Expanding this math to the TLC5940's 12-bit PWM dimming shows that this part is capable of providing a palette of $2^{12} \times 2^{12} \times 2^{12} = 68.7$ billion colors.

PWM dimming is not without its drawbacks. The discrete switching cycles can cause noise in the system. Simultaneously turning on all LEDs at the start of a video frame requires a large inrush current with a very steep rising edge. Without a method to reduce this inrush current, the higher-end LED drivers capable of driving 16 LEDs with up to 120 mA of current in each channel would require excessive input bypass capacitance. Turning on all 16 LEDs simultaneously requires the input capacitor to deliver 1.92 A within the turn-on time of the IC. The upper right graph in Figure 4 shows the ringing present during the leading edge of the current pulse when all LEDs are turned on simultaneously. Parasitic inductance on the PWM creates this noise and ringing. The TLC5940 significantly reduces the effect by staggering the turn-on of each LED. The left side of Figure 4 shows this staggered turn-on. The lower right graph in Figure 4 shows how the staggered turn-on reduces the rise time of the inrush current, which in turn reduces the ringing, the noise in the system, and the input capacitor requirement. The TLC5940 staggers LED turn-off

as well; however, this is not typically needed in most systems. Figure 2 shows that turn-off is inherently staggered when the LEDs are programmed to different dimming levels.

The TLC5940 combines both PWM dimming and dot correction to produce extremely high-quality video. Dot correction produces an accurate LED color by adjusting for changes in an LED's wavelength caused by temperature variations or aging. PWM dimming then provides the shading necessary to provide thousands or millions of individual colors from three individual LEDs. PWM dimming coupled with dot correction is clearly the choice for both existing and future markets requiring high-quality color control in LED-based lighting applications.

Reference

For more information related to this article, you can download an Acrobat Reader file at www-s.ti.com/sc/techlit/litnumber and replace "litnumber" with the **TI Lit. #** for the materials listed below.

Document Title	TI Lit. #
1. Michael Day and Tarek Saab, "TLC5940 dot correction compensates for variations in LED brightness"slyt225

Related Web sites

- power.ti.com
- www.ti.com/sc/device/TLC5940

Wide-input dc/dc modules offer maximum design flexibility

By Geoff Jones (Email: gjones@ti.com)

Marketing Manager

Introduction

When a system designer specifies a nonisolated dc/dc power module, considering the needed input voltage range is equally as important as considering the required performance attributes and features. Generally, nonisolated modules have either a narrow or a wide input voltage range. Narrow-input modules typically have a nominal input voltage of 3.3, 5, or 12 V. For systems that operate from a tightly regulated input bus—such as those that do not use battery backup—a narrow-input module is often adequate since the input remains fairly stable.

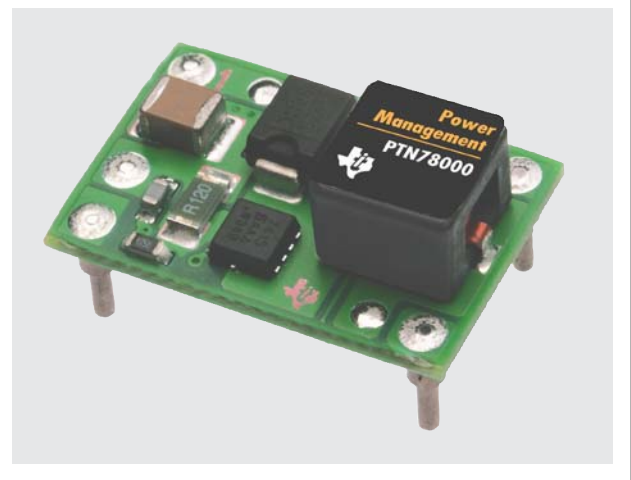
Offering greater flexibility, wide-input modules operate within a range of 7 to 36 V, which includes the popular 12- or 24-V industrial bus. This enables a single module to be used for generating multiple voltages. These modules are ideal for industrial controls, HVAC systems, vehicles, medical instrumentation, and other applications that use a loosely regulated distribution bus. In addition, systems powered by a rectifier/battery charger with lead-acid battery backup almost always require wide-input modules. System designers who choose power supplies may want to take a close look at the latest generation of wide-input dc/dc modules.

What are they?

Wide-input voltage modules are available in three basic types: positive output, positive-to-negative output, and boost output. These modules are designed to operate from a loosely regulated industrial bus input (12 or 24 V nominal) while maintaining a regulated output. Modules from the Texas Instruments (TI) PTN78 series (one of which is shown in Figure 1), for example, accept an input from 7 to 36 V and deliver an output voltage from 2.5 to 12.6 V at 1.5, 3, or 6 A. The output voltage is set with a single external resistor.

Newer wide-input modules are available in double-sided, open-frame construction to minimize cost and weight and to simplify thermal management. The modules are constructed entirely from surface-mount components (including magnetic devices) and are designed for fully automated assembly to help keep manufacturing costs as low as possible. The module's compact packaging yields significant space savings on the PC board and allows the device to be placed close to its load.

Figure 1. TI's PTN78000 module



Wide-input power modules typically integrate input and output capacitors. However, additional input or output capacitors may be needed on the host PC board if there are long input lines to the module coupled with high di/dt requirements or if very low-noise outputs are required.

Most wide-input modules feature an industrial operating temperature range of -40 to $+85^{\circ}\text{C}$. They offer efficiencies as high as 95% and can deliver their full-rated output current at temperatures of up to 60°C with only 200 LFM of airflow.

TI's PTN78 series uses large (up to 0.08-inch-diameter) interconnect pins. The large pins help extend a module's current-carrying capacity so that it requires fewer pins, which saves board space. In the pick-and-place operation during assembly, the module's pins are placed on the PC board along with its other components. This eliminates the need for a secondary pin-attach operation, simplifying assembly.

Wide-input modules also employ built-in functionality such as soft start, on/off inhibit control, current-limit protection, overtemperature protection, and an undervoltage lockout feature to prevent system failure. The devices are available in surface-mount or horizontal through-hole packages. The newer devices like the PTN78 series are designed for RoHS and lead-free compliance.

Input voltage considerations for positive step-down modules

The majority of nonisolated wide-input modules are step-down switching regulators. To keep the output in regulation, the input voltage must exceed the output by a minimum differential voltage due to the limitations of the pulse width modulation (PWM) internal control circuit. This differential voltage can be used to define the maximum advisable ratio between the device's input and output voltages.

As an example, TI's PTN78000W accepts an input from 7 to 36 V and has an adjustable output voltage range from 2.5 to 12.6 V with a single resistor, R_{SET} . Requirements for satisfactory performance of this module are as follows:

- For output voltages lower than 10 V, the minimum input voltage is $(V_O + 2\text{ V})$ or 7 V, whichever is higher.
- For output voltages equal to 10 V and higher, the minimum input voltage is $V_O + 2.5\text{ V}$.
- The maximum input voltage is $(10 \times V_O)$ or 36 V, whichever is less.

Table 1 shows the operating input voltage range for common output bus voltages.

Table 1. PTN78000W standard R_{SET} values for common output voltages

REQUIRED V_O (V)	STANDARD R_{SET} VALUE	ACTUAL V_O (V)	OPERATING V_I RANGE (V)
2.5	Open	2.5	7 to 25
3.3	78.7 k Ω	3.306	7 to 33
5	21 k Ω	4.996	7 to 36
12	732 Ω	12.002	14.5 to 36

Positive-to-negative modules

Positive-to-negative, wide-input modules are buck-boost switching regulators that accept a positive input voltage and produce a negative dc output voltage. The devices are well suited for telecom, industrial tests and measurement, instrumentation, distributed power, and general-purpose circuits.

Latest-generation modules like TI's PTN78000A provide high-efficiency, positive-to-negative voltage conversion for loads of up to 1.5 A. The module has a wide input voltage range of 7 to 29 V and an adjustable wide output voltage range of -3.3 to -15 V. The output voltage is set with a single external resistor.

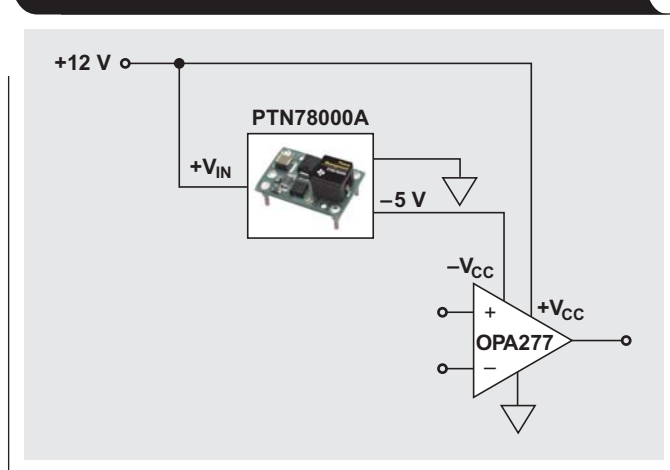
To ensure that the output remains in regulation, the input voltage must not exceed the output by a maximum differential voltage. For satisfactory performance, the maximum operating input voltage is $32 - |V_O|$. As an example, Table 2 gives the operating input voltage range for common bus output voltages.

Some operational amplifiers require positive and negative operating voltage. Figure 2 shows a PTN78000A module converting a +12-V input to a regulated -5-V output to an op amp.

Table 2. Positive step-down module standard R_{SET} values for common output voltages

REQUIRED V_O (V)	STANDARD R_{SET} VALUE	ACTUAL V_O (V)	OPERATING V_I RANGE (V)
-15	100 Ω	-14.997	9 to 17
-12	2 k Ω	-12.006	9 to 20
-5	28.7 k Ω	-5.000	9 to 27
-3.3	221 k Ω	-3.303	9 to 28.7

Figure 2. Positive-to-negative voltage conversion in an operational amplifier application



Boost modules

Boost modules provide high-efficiency, step-up voltage conversion. They generate a stable output voltage that can be adjusted by an external resistor divider. For maximum power efficiency, the integrated devices use a switching rectifier based on a PWM controller.

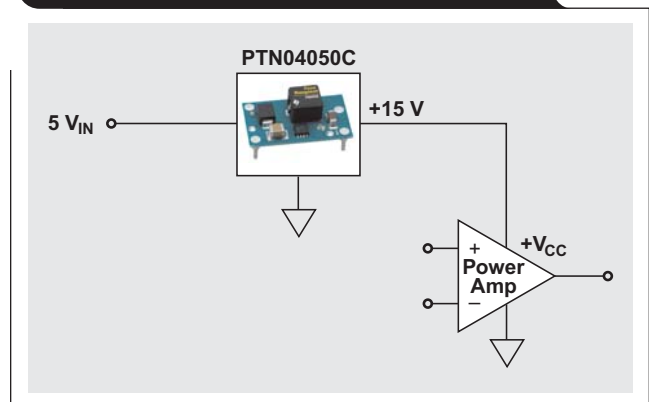
Table 3. Boost module standard R_{SET} values for common output voltages

REQUIRED V_0 (V)	STANDARD R_{SET} VALUE	ACTUAL V_0 (V)	OPERATING V_I RANGE (V)
5.0	Open	5.00	2.9 to 4.5
9.0	4.53 k Ω	9.01	2.9 to 5.5
12.0	1.33 k Ω	12.03	2.9 to 5.5
15.0	60.4 k Ω	14.99	2.9 to 5.5

TI's PTN04050C is a boost module designed for use with 3.3- or 5-V bus systems that require an additional regulated 5 to 15 V with up to 12 W of output power. The output voltage is set with a single external resistor and may be set to any value within the 5- to 15-V range. The output voltage can be as little as 0.5 V higher than the input, allowing an output voltage of 5 V with an input voltage of 4.5 V. Table 3 shows standard resistor values for several common output voltages, along with the actual output voltage that the value provides.

Target applications for boost modules include telecom, industrial tests and measurement, instrumentation, distributed power, and general-purpose circuits. With the

Figure 3. Boost module providing step-up voltage conversion for a power amplifier



ability to operate from 3.3- or 5-V bus systems, a boost module can be used together with a positive step-down module to create plus and minus voltage rails required by many analog ICs such as op amps and data converters.

The module in Figure 3 is shown operating from a +5-V input and producing a +15-V output to a power amplifier.

What's available?

The number of wide-input modules introduced to the marketplace is growing. The wide product choice facilitates precise application matching and simplifies migration to higher-current modules when needed. Table 4 lists some of the products available from TI.

Table 4. TI's wide-input, nonisolated dc/dc modules

DESCRIPTION	MODEL	INPUT VOLTAGE (V)	OUTPUT VOLTAGE (V)	OUTPUT CURRENT	PACKAGE
Positive Step-Down	PTN78000W/H	7 to 36	2.5 to 12.6/12 to 22	1.5 A	SMD, TH
	PTN78060W/H	7 to 36	2.5 to 12.6/12 to 22	3 A	SMD, TH
	PTN78020W/H	7 to 36	2.5 to 12.6/12 to 22	6 A	SMD, TH
Positive to Negative	PTN04050A	+2.9 to +7	-3.3 to -15	1 A (6 W)	SMD, TH
	PTN78000A	+7 to +29	-3.3 to -15	1.5 A (9 W)	SMD, TH
	PTN78060A	+9 to +29	-3.3 to -15	3 A (15 W)	SMD, TH
	PTN78020A	+9 to +29	-3.3 to -15	4 A (25 W)	TH
Positive Boost	PTN04050C	2.9 to 5.5	5 to 15	1 A (12 W)	SMD, TH

The ultimate in design flexibility

TI's wide-input modules provide system designers increased migration-path flexibility to accommodate evolving system power requirements. The wide-input range and output voltage combinations eliminate redesign of an existing power architecture when voltage requirements change. The following system examples show that wide-input modules are suitable for a variety of applications.

Vending machines

Wide-input modules are ideal for vending-machine applications. Vending machines connected to a wireless network help vending-machine managers perform remote diagnostics, monitor inventory levels, schedule service calls, and track real-time sales through a wireless interface. Sending data via a cell phone within each vending machine provides an instant snapshot of the user's entire vending system.

As shown in Figure 4, the wide-input modules accept the loosely regulated output (18 to 32 V) from the vending

machine's inexpensive ac/dc converter. One module is providing a 12-V/1.5-A output for the cell phone; the other is providing a 5-V/3-A output for the displays and logic PC board. Modules that can operate in an environment of -40 to +85°C are ideal for vending equipment that is placed outdoors and are effective for embedded applications in industrial and other challenging environments.

Security cameras

Wide-input modules simplify power management in security cameras. Figure 5 shows a typical power-management circuit powered by a wall-mount ac/dc adapter. A 24-V battery is used to provide emergency backup power. Because of the wide output voltage tolerance of the 24 V from the ac/dc adapter, the circuit requires dc/dc modules capable of operating over a wide input voltage range.

The wide-input modules in Figure 5 are shown operating from a 24-V input. One module is providing a 12-V output to a motor control circuit for the camera's focus and zoom

Figure 4. Vending-machine application

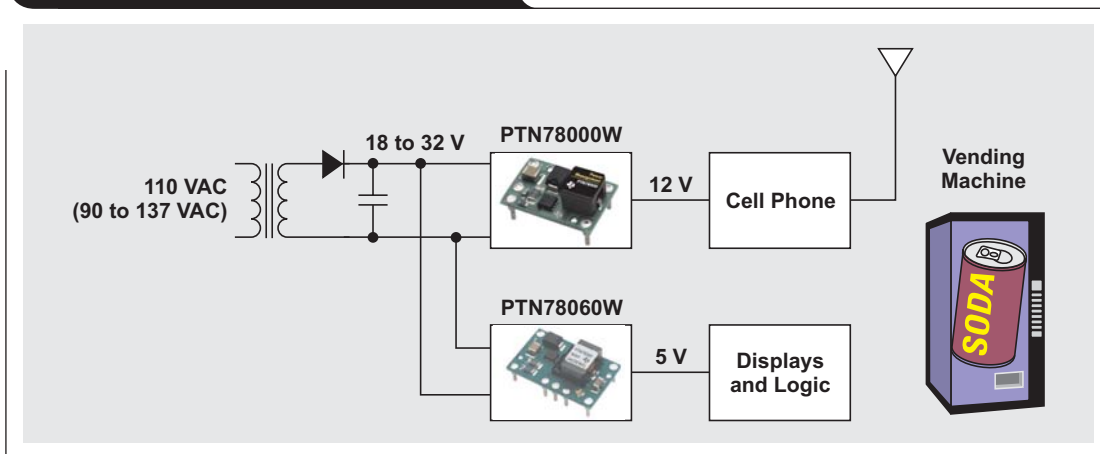


Figure 5. Security-camera application

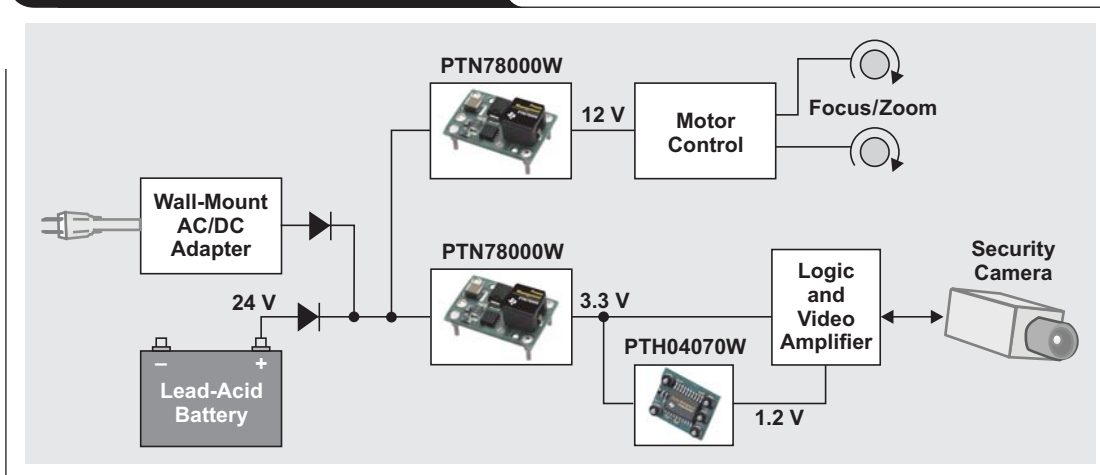
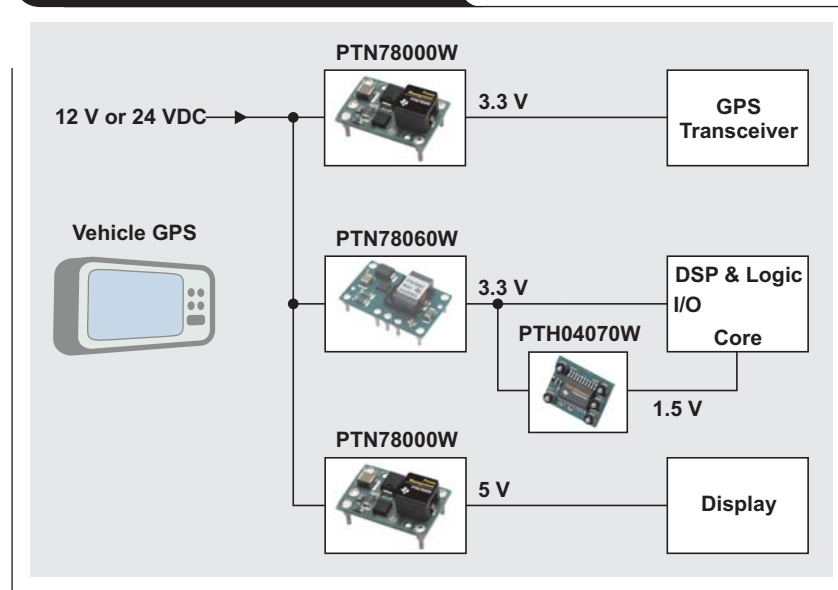


Figure 6. Vehicle GPS application

functions. The other module is providing a 3.3-V output to a video amplifier and a nonisolated module, which is producing a 1.2-V output for a DSP's core voltage.

Vehicle GPS systems

Wide-input modules provide high-efficiency, step-down voltage conversion for a wide variety of vehicle GPS navigation systems. Aftermarket dash-mount GPS systems such as those from Garmin, Magellan, and other manufacturers are popular applications. There are also marine GPS systems and golf carts that use GPS-based range finders. More advanced applications include commercial truck and rail-car monitoring systems. These small, self-contained units, about the size of a paperback novel, have no display. They consist of a black box that enables a central tracking center to monitor the position of entire fleets or rail cars.

As shown in Figure 6, vehicle GPS systems need to be powered by either 12 V (in a car) or 24 V (in a truck or bus). One module provides a 3.3-V/1.5-A output to a GPS transceiver and a 5-V/1.5-A output to the LCD display. The other module provides a 3.3-V/3-A output for the DSP's I/O voltage. It also powers a nonisolated module that delivers a 1.5-V/3-A output for the core voltage.

Purchasing flexibility

The commercial availability of wide-input modules offers purchasing flexibility. Leading distributors provide samples and production quantities in volume for quick design qualification or last-minute changes. Numerous output

voltage and current combinations as well as package options are offered.

Large OEMs prefer to work with a small base of approved suppliers to keep costs down. With a wide input voltage range and adjustable output, one module can be used in a variety of applications. Using fewer modules reduces the number of parts that OEMs must keep in stock.

Summary

System designers are employing increasing numbers of nonisolated dc/dc power modules in their designs. Wide-input, nonisolated modules provide precise power at the load and a great deal of flexibility, helping system designers cope with changes in power requirements. These modules provide all the active functions for local dc/dc conversion with fast transient response and accurate regulation in the smallest possible PC board area. Their wide operating voltage range makes them ideal for industrial, battery-powered, and advanced computing and server applications that use a loosely regulated distribution bus.

Related Web sites

power.ti.com

www.ti.com/sc/device/partnumber

Replace *partnumber* with PTH04070W, PTN04050A, PTN04050C, PTN78000A, PTN78000H, PTN78000W, PTN78020A, PTN78020H, PTN78020W, PTN78060A, PTN78060H, or PTN78060W

Powering today's multi-rail FPGAs and DSPs, Part 2

By Jeff Falin (Email: j-falin1@ti.com)

Power Management Products/Portable Power dc/dc Applications

Introduction

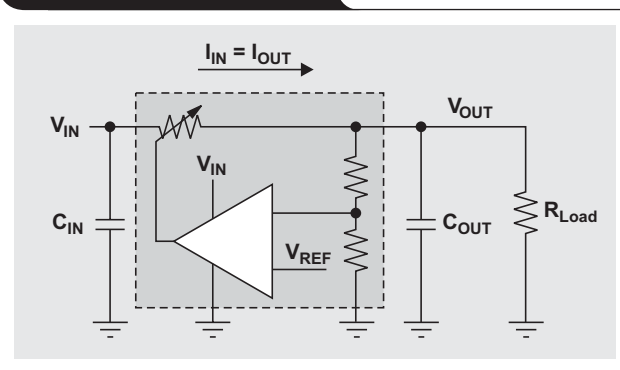
Most electronics have one or more digital processing ICs, such as FPGAs or DSPs, that require multiple power-supply rails. There are various options to consider and potential pitfalls to avoid in powering these digital ICs. This article, Part 2 of a two-part series, provides recommendations and guidance for developing a power solution for multi-rail applications where the input power supply voltage is assumed to be equal to or greater than the system rail voltage (e.g., 12, 5, or 3.3 V). While Part 1 (see Reference 1) discussed system-level concerns such as the power budget and sequencing options, this article focuses on how to choose between the types of point-of-load (POL) dc/dc converters and how to design them to meet dc accuracy, start-up, and transient requirements.

Review of step-down dc/dc converter topologies

There are two types of step-down or “buck” POL dc/dc converters: linear regulators and inductor-based switching regulators. Figure 1 shows the functional diagram of a linear regulator.

The primary benefit of linear regulators is the low cost of their ICs, design time, and board area, since they have

Figure 1. Linear regulator



an internal switch and need only an input and output capacitor. In addition, linear regulators provide a clean, low-noise output voltage. Their primary drawback is low efficiency, equal to V_{OUT}/V_{IN} at heavy load, resulting in a power dissipation of $(V_{OUT}-V_{IN}) \times I_{OUT}$. Power is lost as heat that must be dissipated by the regulator's package and/or external heat sink. Since the minimum input voltage for most regulators currently on the market is 1.8 to 2.7 V, linear regulators are best suited for higher-voltage rails with lower load currents. A second drawback seen in the lowest-cost, featureless regulators is fast, uncontrollable startup, which will be discussed later in this article.

Figure 2. Synchronous buck switching regulator

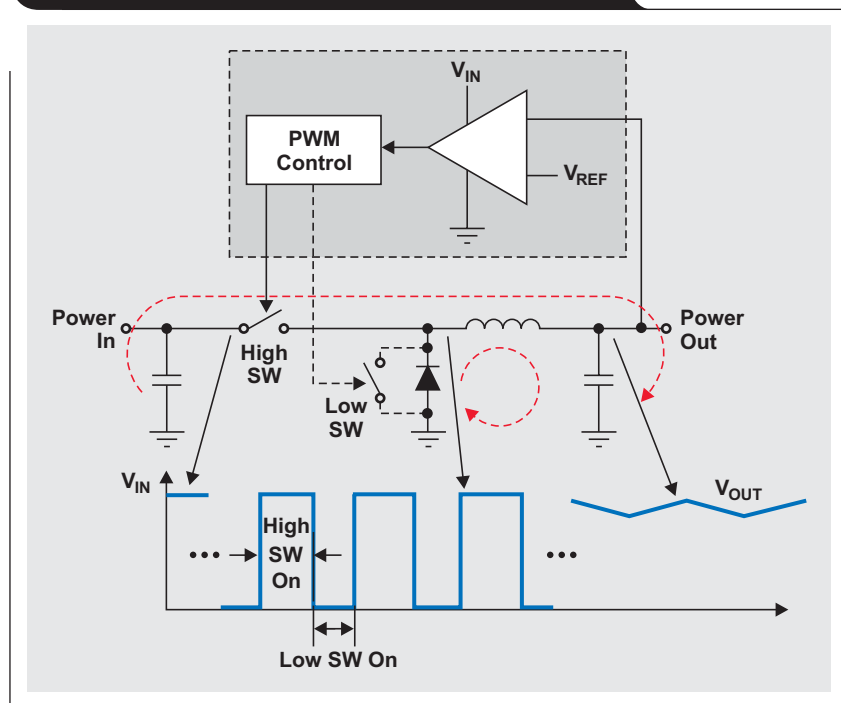


Figure 2 shows a block diagram of a synchronous buck switching regulator. Buck switching regulators use two switches to generate a pulse train with a duty cycle equal to V_{OUT}/V_{IN} . The regulator's feedback control loop modulates either the pulse width of a fixed-frequency pulse train or both the pulse frequency and width to maintain regulation as the load varies, hence the term “pulse width modulation” (PWM). The square-wave pulse train is then filtered by an inductor and capacitor (the LC output filter) to provide a dc output voltage with a triangular-shaped output voltage ripple.

The converter's topology, whether with fixed- or variable-frequency PWM, influences output ripple. The control loop for fixed-frequency PWM converters uses an error amplifier with a negative feedback loop that regulates the output voltage across a load range by modulating the pulse width.

The output ripple of these regulators is formed by the product of the inductor ripple current and the output capacitor's equivalent series resistance (ESR). Thus, choosing a larger inductor than necessary and a low-ESR output capacitor minimizes output ripple. However, low-ESR output capacitors make the feedback loop more difficult to compensate. Fortunately, power IC manufacturers provide power-supply design software that greatly reduces the design time for fixed-frequency PWM converters. The control loop for most variable-frequency converters consists of a comparator, with either time or voltage hysteresis, that turns the switch on or off if the output voltage goes respectively below or above the reference voltage. These hysteretic converters require less design time than fixed-frequency converters due to their simplified control loop. In addition, since the comparator turns the switch on almost immediately after the output falls below the comparator's reference voltage, a hysteretic converter may respond faster to current increases (transients) than the fixed-frequency converter with a finite-bandwidth control loop. However, a hysteretic converter requires a minimum output ripple to operate.

Compared to linear regulators, switching converters have much higher efficiency (85 to 95% typically), but the cost of their ICs, support components, design time, and board area is usually higher. Another drawback of switching regulators compared to linear regulators is their switching noise (e.g., EMI) and output ripple. Switching noise can be minimized through careful component selection, such as shielded inductors and low-ESR output capacitors, and through proper board layout. Hysteretic converters produce output voltage ripple and radiated emissions at variable switching frequencies, which may be difficult to filter. However, when either the output current or the input-to-output differential is large or the input supply has limited power—e.g., an inexpensive wall brick—only a switching converter can provide high enough efficiency to minimize the power lost through heat.

Step-down switching converters are available in various levels of integration. Drop-in modules have limited design

flexibility and tend to cost more; but they require the least amount of design time, needing only an input and output capacitor. At the other extreme are controllers that require external switches as well as the inductor, filter capacitors, and compensation components. They have the most design flexibility and, with enough design effort, can be the most cost-effective solution; but they usually consume the largest amount of board space. In between are the integrated FET buck converters that require less board area, have somewhat less design flexibility, and vary in total solution cost compared to controllers. A synchronous converter/controller uses transistors for both switches and therefore is typically more efficient than a converter that uses a diode for the low-side switch, especially when the output voltage is below 2 V. Therefore, the choice between a linear regulator, a fixed-frequency controller/converter, or a hysteretic controller/converter depends on application requirements as well as on balancing efficiency, cost, and size.

Converter output voltage accuracy

The dc tolerance of most FPGA and DSP core and I/O rails is still $\pm 5\%$; however, tolerances for some core rails as well as power rails for other ICs have dropped to $\pm 3\%$. The lower end of the tolerance range (-5 or -3%) is typically the minimum voltage at which some performance standard (e.g., DSP operating speed) is guaranteed for a particular IC. The upper end of the range may be close to the IC's absolute maximum operating voltage. Understanding how to compute the dc tolerance for a power supply is critical not only to guarantee performance but also for system reliability. The dc tolerance does not include dips due to load-step transients. A load-step transient occurs when a digital device being powered by the POL converter increases its load-current demand very quickly. The factors that contribute directly to the dc tolerance for a power supply are the reference voltage tolerance, the feedback resistor tolerance, and the IC's line and load regulation specifications. As an example, an excerpt from the datasheet of the TPS54310 adjustable buck switching converter (see Reference 2) is shown in Figure 3.

Figure 3. Excerpt from TPS54310 datasheet

PARAMETER	TEST CONDITIONS	MIN	TYP	MAX	UNIT
CUMULATIVE REFERENCE					
V_{ref} Accuracy		0.882	0.891	0.900	V
REGULATION					
Line regulation ^{(1) (3)}	$I_L = 1.5$ A, $f_s = 350$ kHz, $T_J = 85^\circ\text{C}$			0.07	%V
	$I_L = 1.5$ A, $f_s = 550$ kHz, $T_J = 85^\circ\text{C}$			0.07	
Load regulation ^{(1) (3)}	$I_L = 0$ A to 3 A, $f_s = 350$ kHz, $T_J = 85^\circ\text{C}$			0.03	%A
	$I_L = 0$ A to 3 A, $f_s = 550$ kHz, $T_J = 85^\circ\text{C}$			0.03	

(1) Specified by design

(2) Static resistive loads only

(3) Specified by the circuit used in Figure 10 of TPS54310 datasheet.

Table 1 computes the percentage that the 1.2-V $\pm 5\%$ output can dip during a load transient and still be within regulation, assuming a 5-V $\pm 10\%$ input rail and a 100-mA to 3-A dc output load range. Line regulation and load regulation specifications vary per device, even if those devices are from the same power IC manufacturer, so care must be taken when they are used in a calculation. Most recent converters have voltage feedforward, virtually eliminating the output voltage's dependence on input voltage and making line regulation almost negligible. Load regulation is a function of the power IC's loop gain; higher loop gain gives better load regulation. Note that many converters with fixed output voltages and internal compensation have better output voltage accuracy because the output voltage can be set by trimming the internal feedback resistors.

In the example in Table 1, only 2.843% of 1.2 V or 34.1 mV is available for load transient dip before the output voltage will fall below the -5% minimum tolerance. The capacitor(s) on the power rail must be able to supply this load current until the converter can respond, or the voltage will fall below regulation. Capacitors of various sizes and with low

Table 1. Converter accuracy

CONTRIBUTING FACTOR	COMPUTATION	DROOP (%)
V_{REF} accuracy		-1
1% external feedback resistors	$2 \times (1 - V_{REF}/V_{OUT}) \times TOL$	-0.5
Worst-case output ripple	Design for $V_{OUT(PP)} < 1\% \times V_{OUT}$	-0.5
Line regulation	$(0.07\%/V) \times (5.5 - 4.5) \%$	-0.07
Load regulation	$(0.03\%/A) \times (3 - 0.1) A$	-0.087
Total		-2.157
Remainder for load-transient dips	$(5\% - 2.157\%)$	2.843

series resistance and inductance are paralleled for handling load transients. Sizing of the capacitors for this “decoupling network” and how that affects converter response time is discussed later in this article.

Implementing a controlled monotonic rise of the power rail

The final recommended power-supply design practice to be discussed is monotonic rise at startup, as shown in the top graph of Figure 4.

Figure 4. Start-up voltage and current

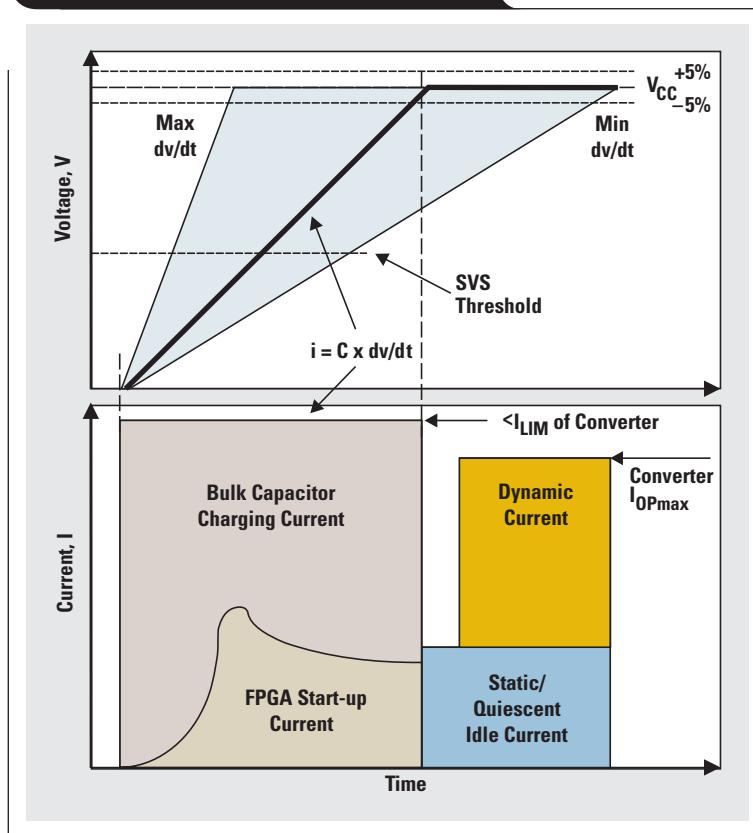
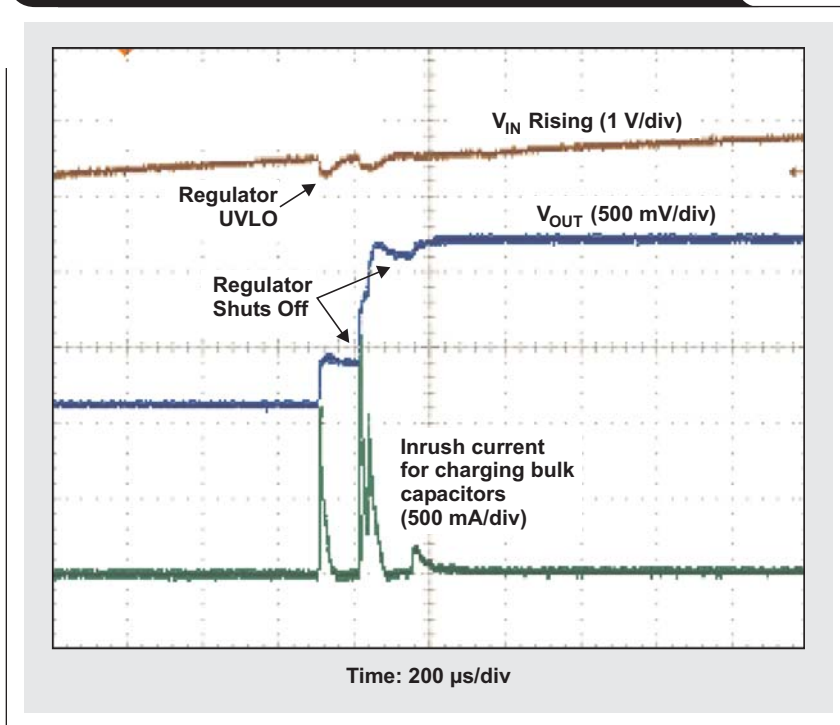


Figure 5. Linear regulator driving a large capacitive load

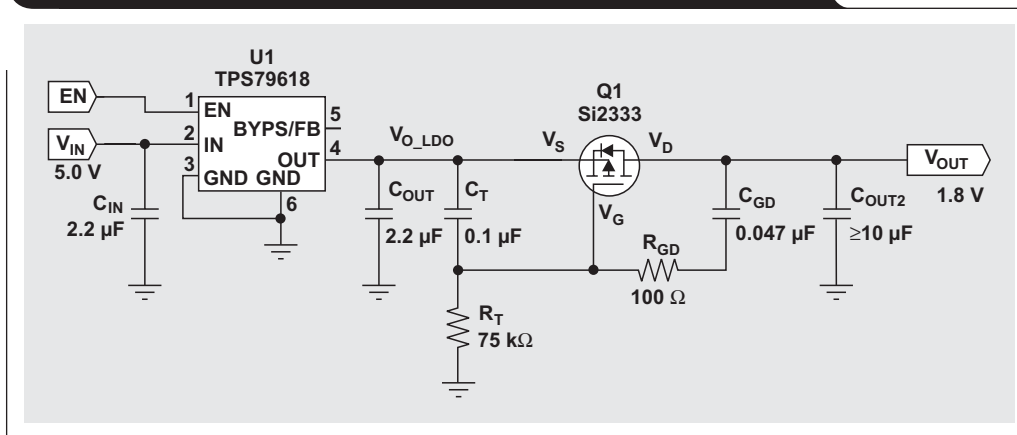


If the bulk capacitance is too large, thereby forcing the POL converter into current limit during startup, there is a risk of the converter cycling in and out of thermal shut-down and thereby never reaching regulation. A more common start-up problem for fast-starting linear regulators occurs when their input supply gets pulled down at startup, temporarily tripping the regulator’s undervoltage lockout (UVLO) until the input capacitor recharges. This causes the regulator to repeatedly turn off briefly and then back on, resulting in the output voltage appearing to oscillate and/or finally ratcheting up to the final voltage. Figure 5 shows an example of a fast-starting linear regulator being powered from a bench supply, pulling the input supply

down, tripping UVLO and turning off, repeating the same cycle, then finally reaching its regulated output voltage.

Few linear regulators have a controllable soft start. At startup, they provide current up to their current limit to charge the output capacitance until they either thermally limit themselves or pull down the input rail as shown in Figure 5. All switching converters have some sort of soft start, whether internally fixed or externally adjustable. A FET following any dc/dc converter can be used as a current-limiting switch to provide a soft start. Figure 6, taken from Reference 3, shows such an application; and Figure 7, also taken from Reference 3, shows the results of soft starting.

Figure 6. Linear regulator with FET following to provide soft start



There are two methods that linear regulators and switching converters commonly use to implement a soft start: reference voltage-controlled or current-limit-controlled. In both, a small external capacitor (in the picofarads to 1- μ F range) controls the soft-start timing. A voltage-controlled soft start is usually implemented by slowly ramping up the reference voltage. Since the feedback loop forces the converter to provide enough current so that the output voltage follows the reference voltage, the output voltage ramps proportional to the soft-start capacitor that is providing the reference voltage during startup. A simple timing equation determines the size of the external capacitor needed to set the dv/dt of the output voltage. Assuming that the inrush current is predominantly for charging bulk capacitors, C_{Bulk} , the inrush current will be fixed, as shown in Figure 4, at $i = C_{Bulk} \times dv/dt$. Ratiometric sequencing, discussed in Part 1 of this series, can be implemented by having two converters with this type of soft start share the same soft-start capacitor. When using a current-limit-controlled soft start, the converter either slowly ramps or incrementally steps up the current limit to the maximum. The converter then looks like a current source, providing a slowly increasing current to the load. The voltage feedback loop still tries to provide the desired output voltage, so the converter provides as much current as the current limit (and any thermal protection) will allow. The output voltage's exact ramp rate, dv/dt , varies as a function of the absolute value of the output voltage (i.e., a 1.2-V rail will ramp more quickly than a 3.3-V rail), the resistive and capacitive loading on the rail, and the converter's final current-limit setting.

Dealing with load-step transients

All POL dc/dc converters have a finite transient response time, whether it's the loop bandwidth of the traditional PWM converter or the fixed on/off times of the hysteretic converter. Figure 8 shows the response of a low-current linear regulator to a change in the output load current—for example, a line of code that causes a DSP to perform complex computations.

Figure 7. Linear regulator with FET following to provide soft start

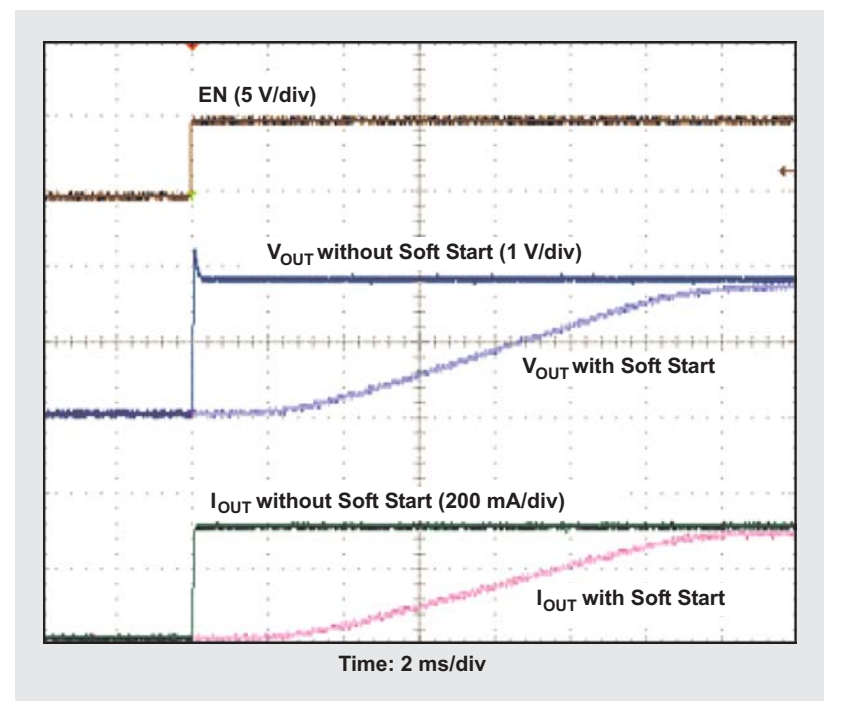


Figure 8. Example load-step transient response

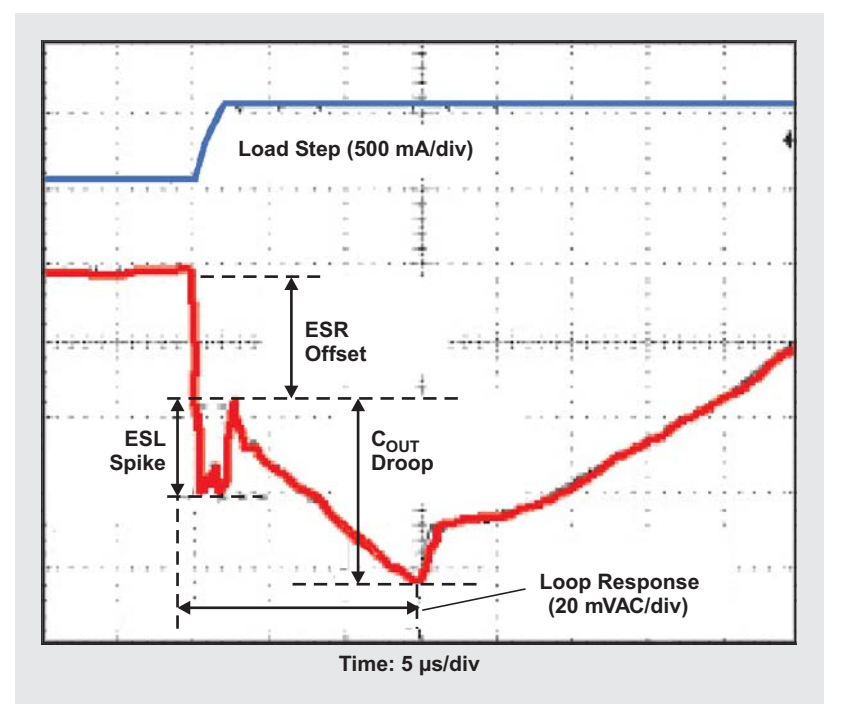
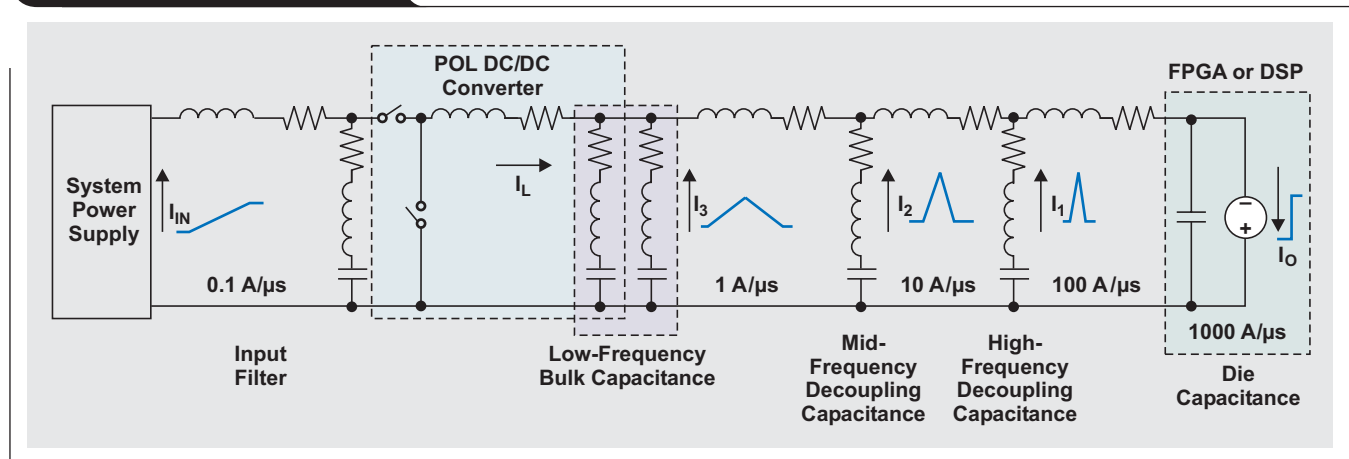


Figure 9. Decoupling network



Using output capacitors with low ESR and equivalent series inductance (ESL) helps to minimize the transient droop. However, additional capacitance is almost always required at the power rail's output and localized bypass capacitance to assist the converter in handling the step transient. Figure 9 shows load-step-transient propagation and its suppression by a decoupling network. The various-sized capacitors suppress the different frequency components of the load-step transient so that the POL converter, and ultimately its input power supply, have to support only the small, low-frequency component of the load step. For example, if the FPGA or DSP gives a load step of $1000 \text{ A}/\mu\text{s}$, then the decoupling network suppresses the transient so that the converter has to respond only to a $1\text{-A}/\mu\text{s}$ transient.

Small capacitors (in the picofarads to $1\text{-}\mu\text{F}$ range) handle the high-frequency component of the load step. Capacitors from 1 to $22 \mu\text{F}$ handle the mid-frequency component, and low-ESR bulk capacitors from 47 to $1000 \mu\text{F}$ handle the low-frequency component. A common method for optimizing the decoupling network (i.e., minimizing the amount of capacitance added) is the target-impedance method, which is explained more fully in Reference 4. This method requires that the designer know the worst-case load-step transient of the device being powered (e.g., from 200 mA to 2.2 A in $0.5 \mu\text{s}$ or $4 \text{ A}/\mu\text{s}$ for $10 \mu\text{s}$) and have some idea of the transient-response capabilities of the POL converter. If the POL converter is not close to the digital IC being powered and/or the board layout requires that the power rail use small traces and/or vias to get to the load, then approximations of the board resistance and inductance may be necessary for the model, as illustrated in Figure 9.

For most FPGA and DSP applications, the worst-case load-step transient is rarely known and it is simpler to use rules of thumb to design the decoupling network. For example, it is not uncommon to allocate a certain percentage of each capacitor type (high-, mid-, and low-frequency) per the number of power pins used in total or per section of the digital IC. While effective, this method tends to overdesign the decoupling network, underutilizing the linear regulator's or switching converter's transient-response capabilities and consuming board space for extra capacitance.

With rule-of-thumb methods, the decoupling network and POL converter are designed independently. This poses a risk that the POL converter may become unstable due to the additional capacitance of the decoupling network; so it is critical that the converter be compensated for the total capacitance at its output. Texas Instruments has reference documents and design software at power.ti.com/swift to assist with converter design and compensation. Artificially applying a load-step transient to the output of the converter and observing the ringing (oscillations) on the output voltage as the converter responds to the transient is another way to determine stability of the converter. As a rule of thumb, if the converter has over three oscillations before settling, it is considered on the verge of being unstable (underdamped). A slow response with no ringing or overshoot is considered to be very stable (overdamped).

PC processors can have multiple load-step transients in the $1000\text{-A}/\mu\text{s}$ range and so require both a fast transient POL converter and a large decoupling network. To reduce the cost of the decoupling network and minimize the

board space it uses, PC motherboard manufacturers now use the target-impedance method or a similar method to minimize the number of capacitors and to take full advantage of the transient capabilities of the dc/dc converter. Individual FPGA and DSP applications are currently lower-power and slower-switching compared to PC processors. So, until either FPGAs or DSPs generate load steps similar to PC processors or the size or cost of the decoupling network becomes too large, a rule-of-thumb approach to sizing the decoupling network is a reasonable compromise between optimal design and fast time to market.

Conclusion

Choosing the right power-supply solution for multi-rail applications is more than balancing size, efficiency, and cost between a linear regulator and the various types of switching converters. Issues such as power-up sequencing and start-up current management must also be considered. In addition, the converter will most likely need the help of decoupling capacitors to maintain regulation during load-step transient events.

References

For more information related to this article, you can download an Acrobat Reader file at www-s.ti.com/sc/techlit/litnumber and replace "litnumber" with the **TI Lit. #** for the materials listed below.

Document Title	TI Lit. #
1. Jeff Falin, "Powering today's multi-rail FPGAs and DSPs, Part 1,"slyt232
2. "3-V to 6-V Input, 3-A Output Synchronous-Buck PWM Switcher with Integrated FETs (SWIFT™)," TPS54310 Datasheetslvs412
3. Jeff Falin, "Monotonic, Inrush Current Limited Start-Up for Linear Regulators," Application Reportslva156
4. "Practical Considerations in Current Mode Power Supplies," Application Reportslua110

Related Web sites

power.ti.com

power.ti.com/swift

www.ti.com/sc/device/TPS54310

www.ti.com/sc/device/TPS79618

Device spacing on RS-485 buses

By Kevin Gingerich (Email: k-gingerich@ti.com)

High-Performance Linear/Interface

The RS-485 bus is a distributed parameter circuit whose electrical characteristics and responses are primarily defined by the distributed inductance and capacitance* along the physical media. The media is defined here as the interconnecting cable(s) or conducting paths, connectors, terminators, and RS-485 devices added along the bus. The following analysis derives a guideline for the amount of capacitance and its spacing that can be added to the bus.

For a starting approximation, the characteristic transmission line impedance at any cut point in the unloaded RS-485 bus is defined by the following equation, where L is the inductance per unit length and C is the capacitance per unit length.

$$Z = \sqrt{\frac{L}{C}}$$

As capacitance is added to the bus in the form of devices and their interconnections, the bus impedance is lowered to Z' , causing an impedance mismatch between the media and the loaded section of the bus.

As the input signal wave arrives at this mismatch in impedance, an attenuation (or amplification) of the signal will occur. The signal voltage at an impedance mismatch is $V_{L1} = V_{L0} + V_{J1} + V_{R1}$, where V_{L0} is the initial voltage, V_{J1} is the input signal voltage, and V_{R1} is the reflected voltage. The voltage reflected back from the mismatch is $V_{R1} = \rho_L \times V_{J1}$, where

$$\rho_L = \frac{Z' - Z}{Z' + Z}$$

and is the coefficient of reflection commonly used in transmission line analysis. The voltage equation can now be written as $V_{L1} = V_{L0} + V_{J1} + \rho_L \times V_{J1}$.

With fast transfer rates and electrically long** media, it becomes essential to achieve a valid input voltage level on the *first* signal transition from an output driver anywhere on the bus. This is called incident-wave switching. If incident-wave conditions are not achieved, reflected-wave switching must be used. To achieve a valid logic voltage level, reflected-wave switching depends upon reflected energy occurring some time after the first transition arrives.

*All capacitances are differential in this article. The differential is approximately one-half of the single-ended capacitance.

**“Electrically long” is defined here as

$$\tau > \frac{t_{10-90\%}}{3}$$

where τ is the one-way time delay across the bus and $t_{10-90\%}$ is the 10-to-90% transition time of the fastest driver output signal.

Assuming that the bus is terminated at both ends with the nominal media impedance and no fail-safe offset, an RS-485 driver will create a high-to-low voltage change from at least 1.5 V to -1.5 V, or a V_{J1} of -3 V. The signal voltage at the load, V_{L1} , should go below the minimum receiver input voltage threshold of -0.2 V.

$$-0.2 > 1.5 + (-3) + \rho_L \times (-3)$$

$$\rho_L > \frac{-0.2 - 1.5 + 3}{-3} = -0.43$$

Now we can solve for Z' :

$$\rho_L = \frac{Z' - Z_0}{Z' + Z_0} > -0.43$$

$$Z' - Z_0 > -0.43(Z' + Z_0)$$

$$Z'(1 + 0.43) > Z_0(1 - 0.43)$$

$$Z' > 0.4Z_0$$

If the loaded bus impedance is no less than $0.4Z_0$, the minimum threshold level should be achieved on the incident wave under all allowed cases.

What bus configuration rules should be used to keep the loaded bus impedance above $0.4Z_0$?

In the derivation of the minimum loaded-bus impedance, we treat the addition of devices and their capacitances in a distributed model. As such, the loaded-bus impedance can be approximated by

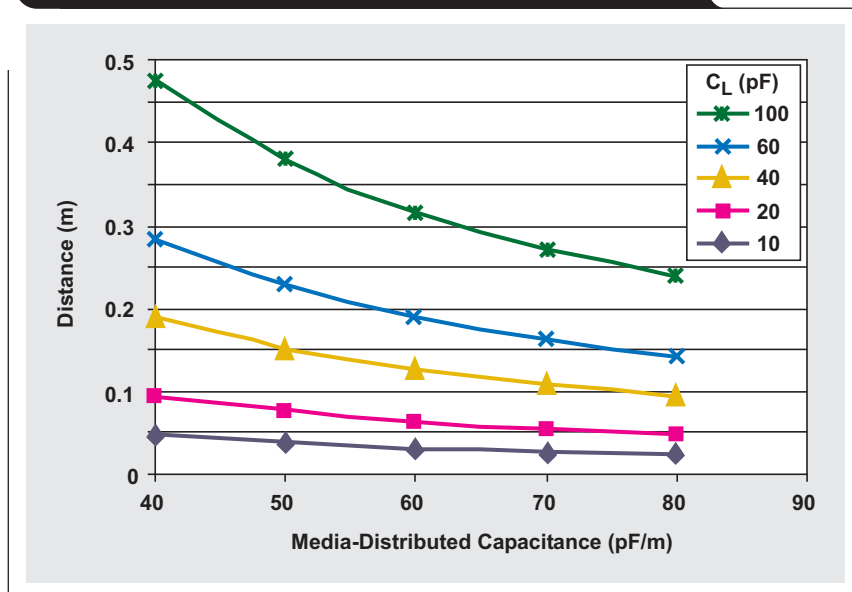
$$Z' = \sqrt{\frac{L}{C + C'}}$$

where C' is the added capacitance per unit length. If we knew the distributed inductance and capacitance of the media, we could calculate Z' directly. Unfortunately, manufacturers do not commonly specify these; but they generally do specify the characteristic impedance, Z_0 , and the capacitance per unit length, C . With these and the relationship

$$Z_0 = \sqrt{\frac{L}{C}}$$

we can solve for L , as $L = Z_0^2 C$. Then we can substitute into the equation for Z' and simplify:

$$Z' = \sqrt{\frac{Z_0^2 C}{C + C'}} = Z_0 \sqrt{\frac{C}{C + C'}}$$

Figure 1. Minimum RS-485 device spacing with device and media capacitance

C' is the distributed device capacitance (C_L) divided by the distance (d) between devices:

$$C' = \frac{C_L}{d}$$

Substituting this into the equation, we can solve for d :

$$Z' = Z_0 \sqrt{\frac{C}{C + \frac{C_L}{d}}}$$

$$\left(\frac{Z'}{Z_0}\right)^2 = \frac{C}{C + \frac{C_L}{d}}$$

$$C \left(\frac{Z_0}{Z'}\right)^2 = C + \frac{C_L}{d}$$

$$d = \frac{C_L}{C \left[\left(\frac{Z_0}{Z'}\right)^2 - 1 \right]}$$

Now substituting our minimum Z' of $0.4Z_0$ gives us d in meters (if C is pF/m) or feet (if C is pF/ft):

$$d > \frac{C_L}{C \left[\left(\frac{Z_0}{0.4Z_0}\right)^2 - 1 \right]}$$

$$d > \frac{C_L}{5.25C}$$

We now have a relationship for the minimum device spacing as a function of the distributed media and lumped-load capacitance. Figure 1 shows this relationship graphically.

Load capacitance includes contributions from the RS-485 line circuit bus pins, connector contacts, printed-circuit-board traces, protection devices, and any other physical connections as long as the distance from the bus to the transceiver is electrically short. RS-485 5-V transceivers, such as the SN65HVD1176, have a capacitance of 7 pF. Transceivers with a 3-V supply, such as the SN65HVD11, have about twice the capacitance that 5-V transceivers have at 16 pF. Board traces add about 0.5 to 0.8 pF/cm depending upon their construction. Connector and suppression device capacitance can vary widely. Media-distributed capacitance ranges from 40 pF/m for low-capacitance, unshielded, twisted-pair cable to 70 pF/m for backplanes.

This derivation gives guidelines for spacing of RS-485 nodes along a bus segment based upon the lumped-load capacitance. The method is equally applicable to other multi-point or multidrop buses, such as CAN, RS-422, or M-LVDS, with appropriate adaptation of the parameter values.

Related Web sites

interface.ti.com

www.ti.com/sc/device/SN65HVD11

www.ti.com/sc/device/SN65HVD1176

Low-cost current-shunt monitor IC revives moving-coil meter design

By Thomas Kugelstadt (Email: tk@ti.com)

Senior Systems Engineer, Industrial Systems

Despite their lack of resolution and accuracy in comparison to digital meters, analog moving-coil meters remain the display of choice when it comes to tracking a reading's trend or drawing information upon a measurement's rate of change. For low-level current measurements, however, the meter current for a full-scale deflection usually exceeds the current to be measured, and a separate supply driving the meter is required. Analog meters of the past, such as the Multavi-10 from Hartmann & Braun, solved this problem by implementing a rechargeable accumulator as the meter supply. Manually selectable shunt resistors in combination with a high-precision chopper amplifier allowed the user to choose from thirteen different current ranges between 1 μ A and 1 A.

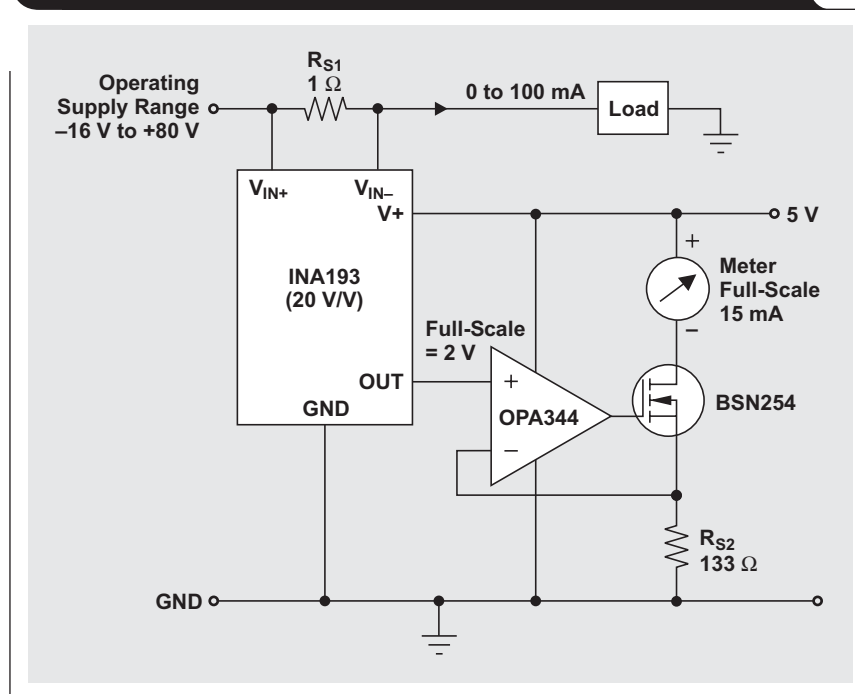
With the introduction of modern current-shunt monitor ICs such as the INA19x family, the amplifier design of moving-coil meters has been drastically simplified. Figure 1 shows the drive circuit of an 8-inch moving-coil meter measuring a current range from 0 to 100 mA. The meter current for a full-scale deflection is 15 mA. The current-shunt monitor, INA193, senses the voltage drop across the 1- Ω shunt resistor, R_{S1} . At a maximum current of 100 mA, the voltage across R_{S1} is 100 mV.

The value chosen for R_{S1} depends on the application and is a compromise between small-signal accuracy and maximum permissible voltage drop in the measurement line. High values of R_{S1} provide better accuracy at lower currents by minimizing the effects of offset, while low values of R_{S1} minimize voltage loss in the supply line. For most applications, the best performance is attained with an R_{S1} value that provides a full-scale shunt voltage range of 50 to 100 mV. The maximum input voltage for accurate measurements is 500 mV.

In this example, the INA193 amplifies the 100-mV full-scale input by a gain factor of 20 V/V, thus providing a full-scale output of 2 V. The succeeding operational amplifier, OPA344, possesses rail-to-rail inputs and outputs; it operates in conjunction with the N-channel MOSFET, BSN254, as a voltage-controlled current source.

Note that the entire meter circuit, including the INA193, operates from a single 5-V supply, which also limits the maximum output voltage swing of the OPA344 to 5 V. It therefore is necessary to choose a MOSFET with a low gate-source threshold voltage, V_{GS} , since this voltage subtracts from the amplifier output swing. The BSN254 has a maximum threshold voltage of 2 V, which satisfies the

Figure 1. Moving-coil meter with separate supply using INA193



low- V_{GS} requirement. Because the voltage at the non-inverting OPA344 input equals the one at the inverting input, the full-scale output of 2 V lies across R_{S2} . To allow for the maximum deflection current to flow, R_{S2} is calculated via

$$R_{S2} = \frac{V_{OUT(FS)}}{I_{Meter(FS)}} = \frac{2 \text{ V}}{15 \text{ mA}} = 133 \ \Omega.$$

R_{S2} can be adjusted to calibrate the meter or to change its full-scale current range. R_{S1} can be adjusted to increase low-current measurement accuracy or to extend the measurement range to higher current values. Another benefit of the circuit is that the meter can be separated from the point of measurement. Because moving-coil meters are not intended for high-precision measurements, the designer can use relaxed-accuracy resistors. Bypassing the instrument supply with decoupling capacitors is necessary to avoid stray pickup from the electrical-noise environment.

About the INA19x current-shunt monitor

The INA193 is just one member of a family of current-shunt monitors. The INA194 and INA195 are members that have the same pinout but provide different gains of 50 V/V and 100 V/V, respectively. Three other current-shunt monitors, the INA196, INA197, and INA198, are functionally identical but come in a different pinout.

The INA19x family uses a new, unique internal circuit topology that provides a common-mode range extending from -16 V to +80 V while operating from a single power supply. The common-mode rejection in a classic instrumentation amplifier approach is limited by the requirement for accurate resistor matching. By converting the induced input voltage to a current, the INA19x provides common-mode rejection that is no longer a function of closely matched resistor values, providing the enhanced performance necessary for such a wide common-mode range.

The simplified diagram in Figure 2 shows the basic circuit function. When the common-mode voltage is positive, amplifier A2 is active. The differential input voltage, $V_{IN+} - V_{IN-}$ applied across R_S , creates the voltage potentials v_N and v_P at A2's inputs:

$$v_N = V_{IN+} - I_S R_S \text{ and } v_P = V_{IN+}.$$

To make $v_P = v_N$, A2 must drive the transistor so that its collector current, I_C , causes a voltage drop across the 5-k Ω resistor that equals the differential input voltage:

$$v_P = v_N$$

$$V_{IN+} - I_C \times 5 \text{ k}\Omega = V_{IN+} - I_S R_S$$

$$I_C \times 5 \text{ k}\Omega = I_S R_S$$

Figure 2. INA19x simplified circuit diagram

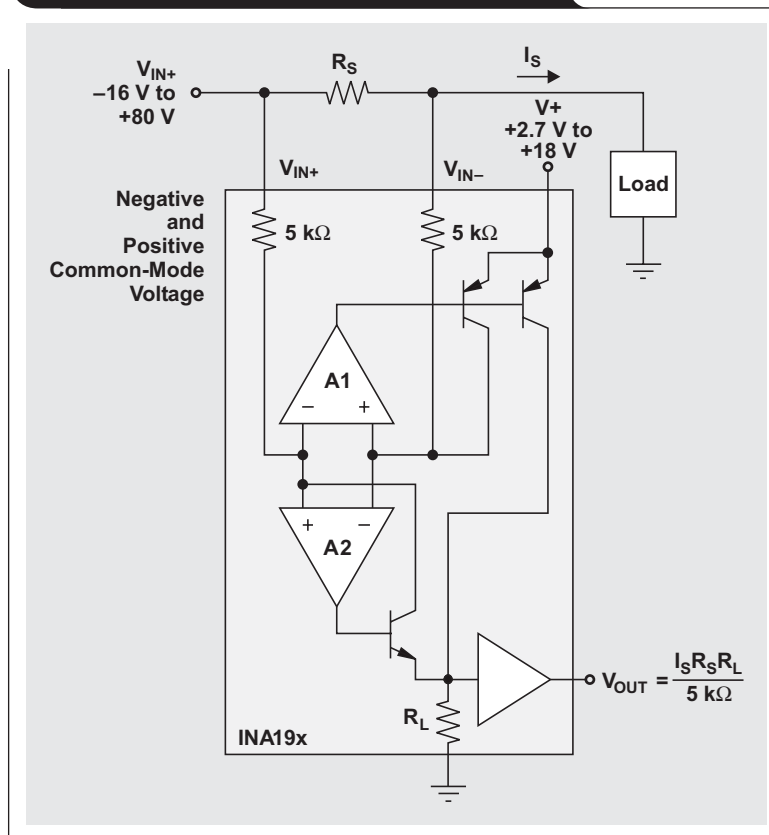
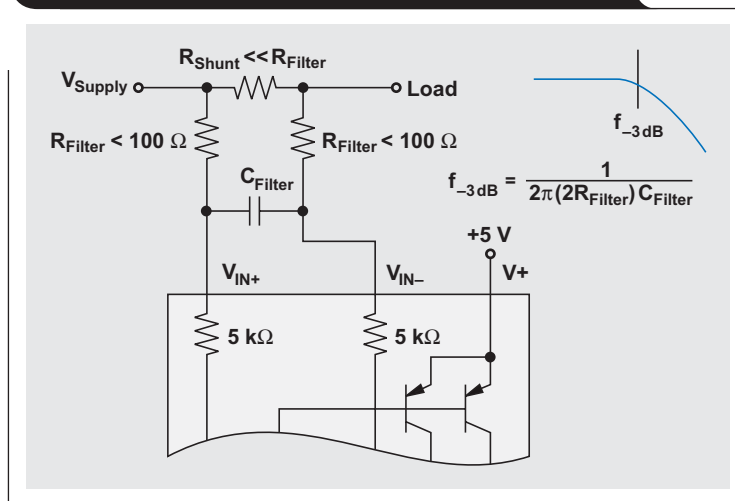


Figure 3. Input filter (gain error = –1.5% to –2.2%)

Expressing I_C through the ratio of output voltage to load resistor,

$$I_C = \frac{V_{OUT}}{R_L},$$

defines the output voltage as

$$V_{OUT} = \frac{I_S R_S R_L}{5 \text{ k}\Omega}.$$

When the common-mode voltage is negative, amplifier A1 is active. The differential input voltage, $V_{IN+} - V_{IN-}$ dropped across R_S , is converted to a current through a 5-k Ω resistor. A1 then drives a precision current mirror whose output through R_L provides the signal voltage to the output buffer amplifier. Patent-pending circuit architecture ensures smooth device operation, even during the transition period when both amplifiers A1 and A2 are active.

The input pins, V_{IN+} and V_{IN-} , should be connected as closely as possible to the shunt resistor to minimize any resistance in series with the shunt resistance. Power-supply bypass capacitors are required for stability. Applications with noisy or high-impedance power supplies may require additional decoupling capacitors to reject power-supply noise. Bypass capacitors should be connected close to the device pins.

The input circuitry of the INA19x can accurately measure beyond its power-supply voltage, $V+$. For example, the $V+$ power supply can be 5 V, whereas the load power-supply voltage is up to +80 V. The output voltage range of the OUT terminal, however, is limited by the voltages on the power-supply pin.

The output of the INA19x is accurate within the output-voltage-swing range set by the power-supply pin, $V+$. This is best illustrated by the INA195 or INA198 (both of which use a gain of 100), where a 100-mV full-scale input from the

shunt resistor requires an output voltage swing of +10 V and a power-supply voltage sufficient to achieve +10 V on the output.

An obvious and straightforward location for filtering is at the output of the INA19x series; however, this location negates the advantage of the internal buffer's low output impedance. The only other option for filtering is at the input pins of the INA19x, which is complicated by the internal input impedance of 5 k Ω + 30% (see Figure 3). Using the lowest possible resistor values minimizes both the initial shift in gain and the effects of tolerance. The effect on initial gain is given by

$$\text{Gain Error \%} = 100 - \left(100 \times \frac{5 \text{ k}\Omega}{5 \text{ k}\Omega + R_{Filter}} \right).$$

Total effect on gain error can be calculated by replacing the 5-k Ω term with 5 k Ω – 30% (or 3.5 k Ω) or 5 k Ω + 30% (or 6.5 k Ω). The tolerance extremes of R_{Filter} can also be inserted into the equation. If a pair of 100- Ω 1% resistors is used on the inputs, the initial gain error will be 1.96%. Worst-case tolerance conditions will always occur at the lower excursion of the internal 5-k Ω (3.5-k Ω) resistor, and at the higher excursion of R_{Filter} – 3% in this case.

Note that the specified accuracy of the INA19x must then be combined in addition to these tolerances. While this discussion has handled accuracy worst-case conditions by combining the extremes of the resistor values, it is appropriate to use geometric mean or root-sum-square calculations to total the effects of accuracy variations.

Related Web sites

amplifier.ti.com

www.ti.com/sc/device/partnumber

Replace *partnumber* with INA193, INA194, INA195, INA196, INA197, INA198, or OPA344

Index of Articles

Title	Issue	Page	Lit. No.
Data Acquisition			
Aspects of data acquisition system design	August 1999	1	SLYT191
Low-power data acquisition sub-system using the TI TLV1572	August 1999	4	SLYT192
Evaluating operational amplifiers as input amplifiers for A-to-D converters	August 1999	7	SLYT193
Precision voltage references	November 1999	1	SLYT183
Techniques for sampling high-speed graphics with lower-speed A/D converters	November 1999	5	SLYT184
A methodology of interfacing serial A-to-D converters to DSPs	February 2000	1	SLYT175
The operation of the SAR-ADC based on charge redistribution	February 2000	10	SLYT176
The design and performance of a precision voltage reference circuit for 14-bit and 16-bit A-to-D and D-to-A converters	May 2000	1	SLYT168
Introduction to phase-locked loop system modeling	May 2000	5	SLYT169
New DSP development environment includes data converter plug-ins	August 2000	1	SLYT158
Higher data throughput for DSP analog-to-digital converters	August 2000	5	SLYT159
Efficiently interfacing serial data converters to high-speed DSPs	August 2000	10	SLYT160
Smallest DSP-compatible ADC provides simplest DSP interface	November 2000	1	SLYT148
Hardware auto-identification and software auto-configuration for the TLV320AIC10 DSP Codec — a “plug-and-play” algorithm	November 2000	8	SLYT149
Using quad and octal ADCs in SPI mode	November 2000	15	SLYT150
Building a simple data acquisition system using the TMS320C31 DSP	February 2001	1	SLYT136
Using SPI synchronous communication with data converters — interfacing the MSP430F149 and TLV5616	February 2001	7	SLYT137
A/D and D/A conversion of PC graphics and component video signals, Part 1: Hardware	February 2001	11	SLYT138
A/D and D/A conversion of PC graphics and component video signals, Part 2: Software and control	July 2001	5	SLYT129
Intelligent sensor system maximizes battery life: Interfacing the MSP430F123 Flash MCU, ADS7822, and TPS60311	1Q, 2002	5	SLYT123
SHDSL AFE1230 application	2Q, 2002	5	SLYT114
Synchronizing non-FIFO variations of the THS1206	2Q, 2002	12	SLYT115
Adjusting the A/D voltage reference to provide gain	3Q, 2002	5	SLYT109
MSC1210 debugging strategies for high-precision smart sensors	3Q, 2002	7	SLYT110
Using direct data transfer to maximize data acquisition throughput	3Q, 2002	14	SLYT111
Interfacing op amps and analog-to-digital converters	4Q, 2002	5	SLYT104
ADS82x ADC with non-uniform sampling clock	4Q, 2003	5	SLYT089
Calculating noise figure and third-order intercept in ADCs	4Q, 2003	11	SLYT090
Evaluation criteria for ADSL analog front end	4Q, 2003	16	SLYT091
Two-channel, 500-kSPS operation of the ADS8361	1Q, 2004	5	SLYT082
ADS809 analog-to-digital converter with large input pulse signal	1Q, 2004	8	SLYT083
Streamlining the mixed-signal path with the signal-chain-on-chip MSP430F169	3Q, 2004	5	SLYT078
Supply voltage measurement and ADC PSRR improvement in MSC12xx devices	1Q, 2005	5	SLYT073
14-bit, 125-MSPS ADS5500 evaluation	1Q, 2005	13	SLYT074
Clocking high-speed data converters	1Q, 2005	20	SLYT075
Implementation of 12-bit delta-sigma DAC with MSC12xx controller	1Q, 2005	27	SLYT076
Using resistive touch screens for human/machine interface	3Q, 2005	5	SLYT209A
Simple DSP interface for ADS784x/834x ADCs	3Q, 2005	10	SLYT210
Operating multiple oversampling data converters	4Q, 2005	5	SLYT222
Low-power, high-intercept interface to the ADS5424 14-bit, 105-MSPS converter for undersampling applications	4Q, 2005	10	SLYT223
Understanding and comparing datasheets for high-speed ADCs	1Q, 2006	5	SLYT231
Matching the noise performance of the operational amplifier to the ADC	2Q, 2006	5	SLYT237

Title	Issue	Page	Lit. No.
Power Management			
Stability analysis of low-dropout linear regulators with a PMOS pass element	August 1999	10	SLYT194
Extended output voltage adjustment (0 V to 3.5 V) using the TI TPS5210	August 1999	13	SLYT195
Migrating from the TI TL770x to the TI TLC770x	August 1999	14	SLYT196
TI TPS5602 for powering TI's DSP	November 1999	8	SLYT185
Synchronous buck regulator design using the TI TPS5211 high-frequency hysteretic controller	November 1999	10	SLYT186
Understanding the stable range of equivalent series resistance of an LDO regulator	November 1999	14	SLYT187
Power supply solutions for TI DSPs using synchronous buck converters	February 2000	12	SLYT177
Powering Celeron-type microprocessors using TI's TPS5210 and TPS5211 controllers	February 2000	20	SLYT178
Simple design of an ultra-low-ripple DC/DC boost converter with TPS60100 charge pump	May 2000	11	SLYT170
Low-cost, minimum-size solution for powering future-generation Celeron™-type processors with peak currents up to 26 A	May 2000	14	SLYT171
Advantages of using PMOS-type low-dropout linear regulators in battery applications	August 2000	16	SLYT161
Optimal output filter design for microprocessor or DSP power supply	August 2000	22	SLYT162
Understanding the load-transient response of LDOs	November 2000	19	SLYT151
Comparison of different power supplies for portable DSP solutions working from a single-cell battery	November 2000	24	SLYT152
Optimal design for an interleaved synchronous buck converter under high-slew-rate, load-current transient conditions	February 2001	15	SLYT139
–48-V/+48-V hot-swap applications	February 2001	20	SLYT140
Power supply solution for DDR bus termination	July 2001	9	SLYT130
Runtime power control for DSPs using the TPS62000 buck converter	July 2001	15	SLYT131
Power control design key to realizing InfiniBand™ benefits	1Q, 2002	10	SLYT124
Comparing magnetic and piezoelectric transformer approaches in CCFL applications	1Q, 2002	12	SLYT125
Why use a wall adapter for ac input power?	1Q, 2002	18	SLYT126
SWIFT™ Designer power supply design program	2Q, 2002	15	SLYT116
Optimizing the switching frequency of ADSL power supplies	2Q, 2002	23	SLYT117
Powering electronics from the USB port	2Q, 2002	28	SLYT118
Using the UCC3580-1 controller for highly efficient 3.3-V/100-W isolated supply design	4Q, 2002	8	SLYT105
Power conservation options with dynamic voltage scaling in portable DSP designs	4Q, 2002	12	SLYT106
Understanding piezoelectric transformers in CCFL backlight applications	4Q, 2002	18	SLYT107
Load-sharing techniques: Paralleling power modules with overcurrent protection	1Q, 2003	5	SLYT100
Using the TPS61042 white-light LED driver as a boost converter	1Q, 2003	7	SLYT101
Auto-Track™ voltage sequencing simplifies simultaneous power-up and power-down	3Q, 2003	5	SLYT095
Soft-start circuits for LDO linear regulators	3Q, 2003	10	SLYT096
UCC28517 100-W PFC power converter with 12-V, 8-W bias supply, Part 1	3Q, 2003	13	SLYT097
UCC28517 100-W PFC power converter with 12-V, 8-W bias supply, Part 2	4Q, 2003	21	SLYT092
LED-driver considerations	1Q, 2004	14	SLYT084
Tips for successful power-up of today's high-performance FPGAs	3Q, 2004	11	SLYT079
A better bootstrap/bias supply circuit	1Q, 2005	33	SLYT077
Understanding noise in linear regulators	2Q, 2005	5	SLYT201
Understanding power supply ripple rejection in linear regulators	2Q, 2005	8	SLYT202
Miniature solutions for voltage isolation	3Q, 2005	13	SLYT211
New power modules improve surface-mount manufacturability	3Q, 2005	18	SLYT212
Li-ion switching charger integrates power FETs	4Q, 2005	19	SLYT224
TLC5940 dot correction compensates for variations in LED brightness	4Q, 2005	21	SLYT225
Powering today's multi-rail FPGAs and DSPs, Part 1	1Q, 2006	9	SLYT232
TPS79918 RF LDO supports migration to StrataFlash® Embedded Memory (P30)	1Q, 2006	14	SLYT233
Practical considerations when designing a power supply with the TPS6211x	1Q, 2006	17	SLYT234
TLC5940 PWM dimming provides superior color quality in LED video displays	2Q, 2006	10	SLYT238
Wide-input dc/dc modules offer maximum design flexibility	2Q, 2006	13	SLYT239
Powering today's multi-rail FPGAs and DSPs, Part 2	2Q, 2006	18	SLYT240

Title	Issue	Page	Lit. No.
Interface (Data Transmission)			
TIA/EIA-568A Category 5 cables in low-voltage differential signaling (LVDS)	August 1999	16	SLYT197
Keep an eye on the LVDS input levels	November 1999	17	SLYT188
Skew definition and jitter analysis	February 2000	29	SLYT179
LVDS receivers solve problems in non-LVDS applications	February 2000	33	SLYT180
LVDS: The ribbon cable connection	May 2000	19	SLYT172
Performance of LVDS with different cables	August 2000	30	SLYT163
A statistical survey of common-mode noise	November 2000	30	SLYT153
The Active Fail-Safe feature of the SN65LVDS32A	November 2000	35	SLYT154
The SN65LVDS33/34 as an ECL-to-LVTTL converter	July 2001	19	SLYT132
Power consumption of LVPECL and LVDS	1Q, 2002	23	SLYT127
Estimating available application power for Power-over-Ethernet applications	1Q, 2004	18	SLYT085
The RS-485 unit load and maximum number of bus connections	1Q, 2004	21	SLYT086
Failsafe in RS-485 data buses	3Q, 2004	16	SLYT080
Maximizing signal integrity with M-LVDS backplanes	2Q, 2005	11	SLYT203
Device spacing on RS-485 buses	2Q, 2006	25	SLYT241
Amplifiers: Audio			
Reducing the output filter of a Class-D amplifier	August 1999	19	SLYT198
Power supply decoupling and audio signal filtering for the Class-D audio power amplifier	August 1999	24	SLYT199
PCB layout for the TPA005D1x and TPA032D0x Class-D APAs	February 2000	39	SLYT182
An audio circuit collection, Part 1	November 2000	39	SLYT155
1.6- to 3.6-volt BTL speaker driver reference design	February 2001	23	SLYT141
Notebook computer upgrade path for audio power amplifiers	February 2001	27	SLYT142
An audio circuit collection, Part 2	February 2001	41	SLYT145
An audio circuit collection, Part 3	July 2001	34	SLYT134
Audio power amplifier measurements	July 2001	40	SLYT135
Audio power amplifier measurements, Part 2	1Q, 2002	26	SLYT128
Amplifiers: Op Amps			
Single-supply op amp design	November 1999	20	SLYT189
Reducing crosstalk of an op amp on a PCB	November 1999	23	SLYT190
Matching operational amplifier bandwidth with applications	February 2000	36	SLYT181
Sensor to ADC — analog interface design	May 2000	22	SLYT173
Using a decompensated op amp for improved performance	May 2000	26	SLYT174
Design of op amp sine wave oscillators	August 2000	33	SLYT164
Fully differential amplifiers	August 2000	38	SLYT165
The PCB is a component of op amp design	August 2000	42	SLYT166
Reducing PCB design costs: From schematic capture to PCB layout	August 2000	48	SLYT167
Thermistor temperature transducer-to-ADC application	November 2000	44	SLYT156
Analysis of fully differential amplifiers	November 2000	48	SLYT157
Fully differential amplifiers applications: Line termination, driving high-speed ADCs, and differential transmission lines	February 2001	32	SLYT143
Pressure transducer-to-ADC application	February 2001	38	SLYT144
Frequency response errors in voltage feedback op amps	February 2001	48	SLYT146
Designing for low distortion with high-speed op amps	July 2001	25	SLYT133
Fully differential amplifier design in high-speed data acquisition systems	2Q, 2002	35	SLYT119
Worst-case design of op amp circuits	2Q, 2002	42	SLYT120
Using high-speed op amps for high-performance RF design, Part 1	2Q, 2002	46	SLYT121
Using high-speed op amps for high-performance RF design, Part 2	3Q, 2002	21	SLYT112
FilterPro™ low-pass design tool	3Q, 2002	24	SLYT113
Active output impedance for ADSL line drivers	4Q, 2002	24	SLYT108
RF and IF amplifiers with op amps	1Q, 2003	9	SLYT102
Analyzing feedback loops containing secondary amplifiers	1Q, 2003	14	SLYT103
Video switcher using high-speed op amps	3Q, 2003	20	SLYT098
Expanding the usability of current-feedback amplifiers	3Q, 2003	23	SLYT099
Op amp attenuators	4Q, 2003	28	SLYT093
Calculating noise figure in op amps	4Q, 2003	31	SLYT094

Title	Issue	Page	Lit. No.
Amplifiers: Op Amps (Continued)			
Op amp stability and input capacitance	1Q, 2004	.24	SLYT087
Integrated logarithmic amplifiers for industrial applications	1Q, 2004	.28	SLYT088
Active filters using current-feedback amplifiers	3Q, 2004	.21	SLYT081
Auto-zero amplifiers ease the design of high-precision circuits	2Q, 2005	.19	SLYT204
So many amplifiers to choose from: Matching amplifiers to applications	3Q, 2005	.24	SLYT213
Instrumentation amplifiers find your needle in the haystack	4Q, 2005	.25	SLYT226
High-speed notch filters	1Q, 2006	.19	SLYT235
Low-cost current-shunt monitor IC revives moving-coil meter design	2Q, 2006	.27	SLYT242
General Interest			
Synthesis and characterization of nickel manganite from different carboxylate precursors for thermistor sensors	February 2001	.52	SLYT147
Analog design tools	2Q, 2002	.50	SLYT122

TI Worldwide Technical Support

Internet

TI Semiconductor Product Information Center Home Page
support.ti.com

TI Semiconductor KnowledgeBase Home Page
support.ti.com/sc/knowledgebase

Product Information Centers

Americas

Phone +1(972) 644-5580
Fax +1(972) 927-6377
Internet/Email support.ti.com/sc/pic/americas.htm

Europe, Middle East, and Africa

Phone
Belgium (English) +32 (0) 27 45 54 32
Finland (English) +358 (0) 9 25173948
France +33 (0) 1 30 70 11 64
Germany +49 (0) 8161 80 33 11
Israel (English) 180 949 0107
Italy 800 79 11 37
Netherlands (English) +31 (0) 546 87 95 45
Russia +7 (0) 95 363 4824
Spain +34 902 35 40 28
Sweden (English) +46 (0) 8587 555 22
United Kingdom +44 (0) 1604 66 33 99
Fax +(49) (0) 8161 80 2045
Internet support.ti.com/sc/pic/euro.htm

Japan

Fax International +81-3-3344-5317
Domestic 0120-81-0036
Internet/Email International support.ti.com/sc/pic/japan.htm
Domestic www.tij.co.jp/pic

Asia

Phone
International +886-2-23786800
Domestic Toll-Free Number
Australia 1-800-999-084
China 800-820-8682
Hong Kong 800-96-5941
India +91-80-51381665 (Toll)
Indonesia 001-803-8861-1006
Korea 080-551-2804
Malaysia 1-800-80-3973
New Zealand 0800-446-934
Philippines 1-800-765-7404
Singapore 800-886-1028
Taiwan 0800-006800
Thailand 001-800-886-0010
Fax +886-2-2378-6808
Email tiasia@ti.com
ti-china@ti.com
Internet support.ti.com/sc/pic/asia.htm

Important Notice: The products and services of Texas Instruments Incorporated and its subsidiaries described herein are sold subject to TI's standard terms and conditions of sale. Customers are advised to obtain the most current and complete information about TI products and services before placing orders. TI assumes no liability for applications assistance, customer's applications or product designs, software performance, or infringement of patents. The publication of information regarding any other company's products or services does not constitute TI's approval, warranty or endorsement thereof.

B120905

Auto-Track, FilterPro, SWIFT and TINA-TI are trademarks of Texas Instruments.
Celeron is a trademark and StrataFlash is a registered trademark of Intel Corporation. All other trademarks are the property of their respective owners.

SLYT236